Rivista Italiana di Paleontologia e Stratigrafia	volume 121	no. 3	2 pls.	pp. 297-327	November 2015

CALCAREOUS NANNOFOSSIL BIOSTRATIGRAPHY AND PALEOCEANOGRAPHY OF THE TOARCIAN OCEANIC ANOXIC EVENT AT COLLE DI SOGNO (SOUTHERN ALPS, NORTHERN ITALY)

CRISTINA EMANUELA CASELLATO & ELISABETTA ERBA

Received: February 03, 2015; accepted: June 16, 2015

Key words: Calcareous nannofossils, biostratigraphy, paleoecology, paleoceanography, Pliensbachian/Toarcian boundary interval, Toarcian Oceanic Anoxic Event.

Abstract. We present calcareous nannofossil biostratigraphy and abundances for the Upper Pliensbachian-Lower Toarcian interval, including the Toarcian Oceanic Anoxic Event (T-OAE), represented by the Fish Level at Colle di Sogno (N Italy). In addition to biohorizons identifying NJT 5 and NJT 6 nannofossil zones, the first occurrences of *C. superbus* and *D. striatus* constrain the onset and the end of the T-OAE, respectively. We propose the last occurrence of *M. jansae* as additional event to approximate the end of the T-OAE at lower latitudes. Quantitative data highlight the "*Schizosphaerella* decline" marking the Pliensbachian/Toarcian boundary and the "*Schizosphaerella* crisis" at the onset of the T-OAE as supplementary biohorizons. *S. punctulata* and *M. jansae* constitute most of the micrite in the interval below the Fish Level, which is marked by an increase in abundance of small coccoliths remaining abundant in the overlying interval, with limited contributions of *S. punctulata,* while *M. jansae* disappears.

Principal Component Analysis implemented nannofossil paleoecological and paleoenvironmental reconstructions. The latest Pliensbachian was characterized by stable oligotrophic conditions favourable to calcification at low pCO_2 levels promoting the proliferation of deep-dwelling and highly-calcified *S. punctulata*. During the earliest Toarcian an initial pulse of continental run-off introduced terrigenous material favouring the intermediate-dweller *M. jansae* and the low-salinity adapted *Calyculus*. Higher nutrient concentrations and ocean acidification magnified during the T-OAE, stimulatying mesotrophic low-calcified coccolith-producers and suppressing k-strategist deep- to intermediate-dwellers. After the T-OAE, partial recovery of calcareous nannoplankton indicates still perturbed conditions. Ecosystem modifications anticipated the T-OAE of ~1 million years with species origination and major changes in assemblages.

Introduction

In the last thirty years, much attention has been devoted to Jurassic calcareous nannofossils to explore their potential as stratigraphic tool for correlations at regional to global scale. During the Early Jurassic, the Late Pliensbachian-Early Toarcian interval was a crucial time for calcareous nannoplankton evolution as a major speciation episode took place and some of the most common Jurassic and Cretaceous genera (*Biscutum, Lotharingius, Discorhabdus* and *Watznaueria*) appeared and rapidly evolved (Bown 1987; Mattioli & Erba 1999; Bown et al. 2004; Erba 2004, 2006) providing a number of biostratigraphic events. The Early Jurassic world was characterized by nannoplankton paleoprovincialism (Bown 1987, 1992; Baldanza et al. 1995) and, therefore, two different biostratigraphic schemes were proposed: a Boreal biozonation based on Northern Europe sections (UK, Germany, The Netherlands) (Bown 1987; Bown et al. 1988; Bown & Cooper 1998) and a Tethyan biozonation based on lower latitude sections (Italy, W Portugal, Central Hungary, SW Germany, S France, Greece) (Mattioli & Erba 1999).

The latest Plienbachian to Early Toarcian time interval was marked by paleoclimatic and paleoceanographic perturbations, associated to transient and long-lasting C isotope anomalies, including the Toarcian Oceanic Anoxic Event (T-OAE) (Jenkyns 1988, 2003, 2010; Hesselbo et al. 2000).

Dipartimento di Scienze della Terra "A.Desio", Università degli Studi di Milano, via Mangiagalli 34, 20133 Milano, Italy.
E-mail: cristina.casellato@unimi.it; elisabetta.erba@unimi.it

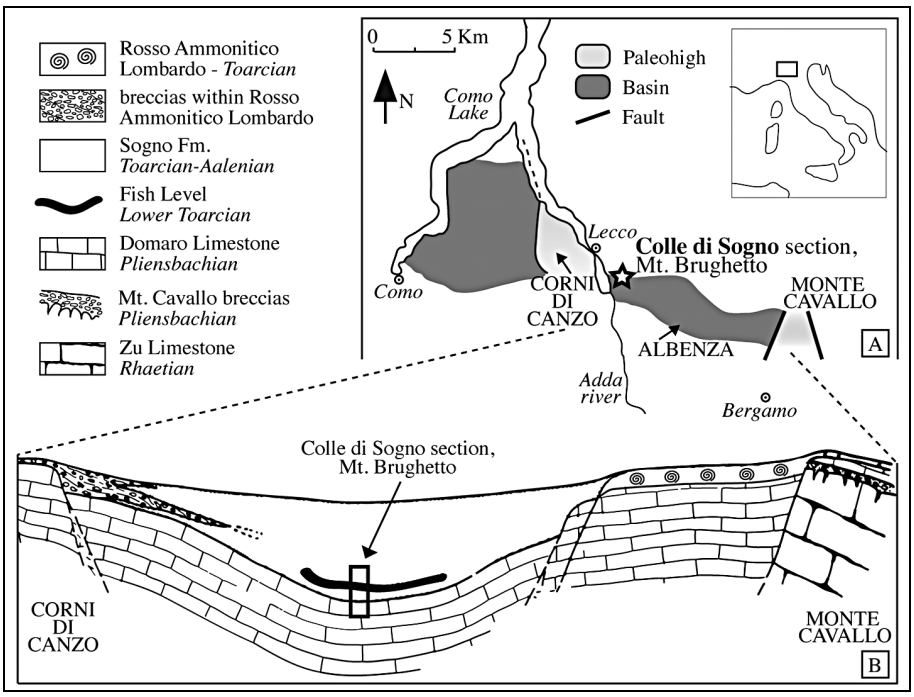

Fig. 1 - A) Distribution of basins and pelagic highs in the central portion of the Lombardy Basin, Southern Alps, during the Early Jurassic (modified from Mattioli & Erba 1999); B) Depositional environment of the Sogno Fm. in the Albenza area (from Gaetani & Poliani 1978).

The high number of calcareous nannofossil biohorizons characterizing the Late Pliensbachian-Early Toarcian time interval offers the opportunity to biostratigraphically constraint the T-OAE. We investigated calcareous nannofossil assemblages of the Colle di Sogno section (Upper Pliensbachian–Lower Toarcian interval), located in the Lombardy Basin within the Southern Alps. This section was previously studied for lithostratigraphy (Gaetani & Poliani 1978) and nannofossil content (Erba 2004). Jenkyns & Clayton (1986) documented low-resolution carbon and oxygen isotopic profiles for the uppermost Pliensbachian-lowermost Toarcian interval, including the T-OAE organic-rich sediments.

The objectives of this study are: A) nannofossil biostratigraphy for dating the Colle di Sogno section and making comparisons with available data to assess biohorizon reproducibility at regional to global scales; B) nannofossil quantitative abundances and statistical analyses for reconstruction of paleoecological affinities and paleoceanographic conditions preceding, during and following the T-OAE perturbation.

Geological Setting and Lithostratigraphy

The studied area is situated in the Southern Alps (N Italy) (Fig. 1A) that in the Mesozoic were part of the southern Tethyan passive margin, belonging to an African promontory, the Adria microplate (Fig. 2). During the latest Triassic-earliest Jurassic time interval this margin experienced an intense rifting that generated a series of structural highs and lows, namely the Lombardy Basin, the Trento Plateau, the Belluno Basin and the Friuli Platform. Within the Lombardy Basin, this tectonic phase further differentiated deep basins and pelagic structural highs, bounded by synsedimentary faults that ruled facies distribution (Winterer & Bosellini 1981; Baumgartner et al. 2001). In the deeper parts sedimentary successions are thick, continuous and temporarily characterized by a pelagic turbiditic regime, whereas condensed and partially discontinuous sedimentation characterizes the pelagic highs.

This study was conducted on the Colle di Sogno section located in the depocentre of the Albenza Plateau (Fig. 1B), where a continuous Jurassic sequence is exposed (Muttoni et al. 2005). In particular, we focus on the Upper Pliensbachian-Lower Toarcian interval (Fig. 3), previously characterized for lithostratigraphy, biostratigraphy and chemostratigraphy (Gaetani & Poliani 1978; Jenkyns & Clayton 1986; Lozar 1995; Mattioli & Erba 1999; Erba 2004), therefore providing an integrated stratigraphic framework for calibration of nannofossil biohorizons and zones. The ammonites (*Dactyloceras simplex* Fucini and *Partschyceras anonymum* Haas) from the top of Domaro Limestone (Lmst.) correspond to the *tenuicostatum* ammonite Zone (AZ) (Gaetani & Poliani 1978). A few ammonite specimens (*Dactylioceras polymorphum* Fucini and *Hildaites* sp. ind.) found approximately one meter above the top of the Fish Level (Gaetani & Poliani 1978) suggest the *falciferum* AZ as discussed by Jenkyns et al. (1985), who interpreted *Dactilioceras* specimens as reworked.

Low-resolution $\delta^{13}C$ data of Jenkyns & Clayton (1986) document a negative shift at the Domaro Lmst./Sogno Formation (Fm.) boundary. Such an anomaly was recognized in different stratigraphic settings and dated as Pliensbachian/Toarcian boundary in recent pa-

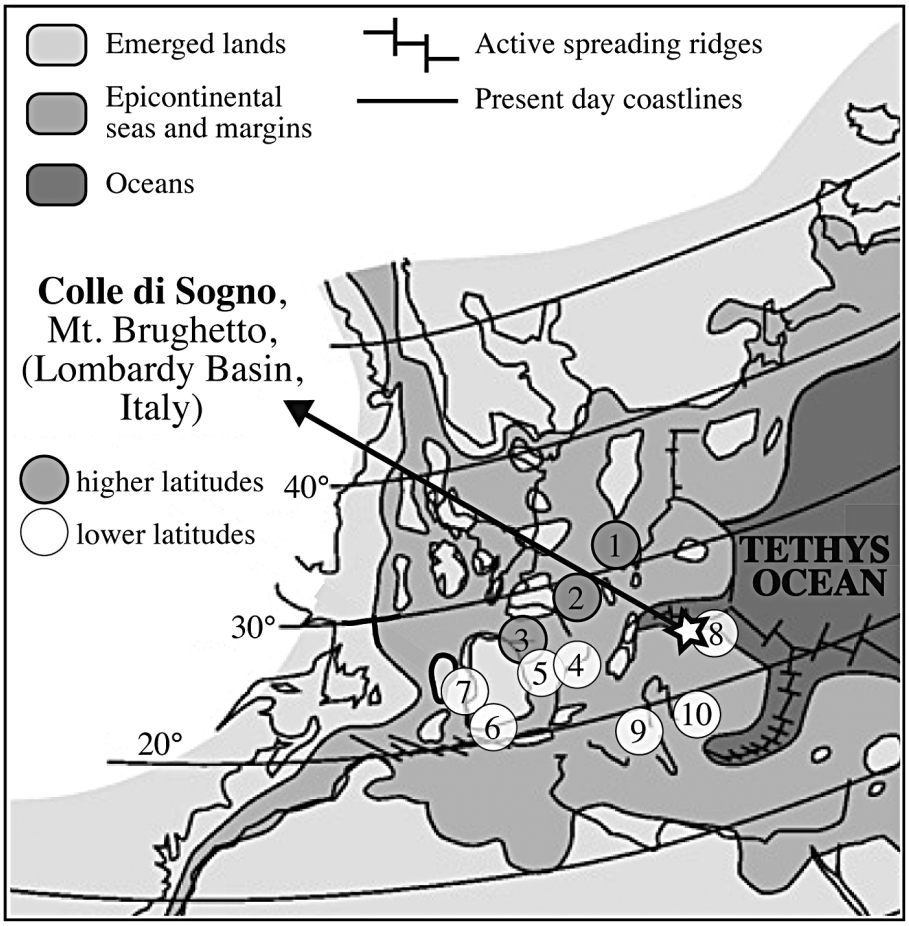

Fig. 2 - Paleogeography of the Early Toarcian (modified from Bassoullet et al. 1993). Numbers represent the paleopositions of the stratigraphic sections cited in Figs 6, 7 and Tab. 1.
1) Dotternhausen - Germany; 2) Sancerre-Couy drill-core - N France; 3) West Rodiles, Camino, San Andrés, Castillo De Pedroso - N Spain; 4) Quercy - SW France; 5) Rambla del Salto; La Almunia - E Spain; 6) La Cerradura - S Spain; 7) Rabacal, Peniche - Portugal; 8) Colle di Sogno, Caricatore, Val Varea - N Italy; 9) Pozzale, Colle D'Orlando, Fonte Cerro, Valdorbia, Mt. Serrone, Mt. Civitella, Somma - Central Italy; 10) Anabrisada, Kaballos, Kalamisti, Toka - NW Greece. Sections at higher paleolatitudes (1-3) are distinguished from sections at lower paleolatitudes (4-10).

pers (Hesselbo et al. 2007; Suan et al. 2008, 2010), and thus reinforces the age assignment based on ammonites of the topmost layer of the Domaro Lmst. Another negative excursion grossly correlates with the Fish Level: this is the widely recognized carbon isotope excursion associated with the T-OAE, and suggests that the Fish Level is the local sedimentary expression of this event.

The studied ~30 m-thick interval, spanning the uppermost part of the Domaro Lmst. and the lowermost part of the Sogno Fm. (Fig. 3) is located along the road SP 179 leading northward from the village of Sogno to Colle di Sogno, on the northern slope of Mt. Brughetto (45°47'29" N, 9°28'44" E). The Domaro Lmst. consists of light grey marly limestone and limestone in 25-15 cm-thick beds, with greenish marly claystone interbeds, which sometimes reach a thickness up to 5 cm. Rare grey cherts nodules and lists, 1-2 cm-thick, are present. The lithostratigraphic boundary with the Sogno Fm. is sharp and marked by the occurrence of a 27 cm-thick interval of greenish marly claystone. The lower 8.27 m of the Sogno Fm. consists of greenish and reddish marlstone and limy marlstone in 25 to 5 cm-thick beds. A slumped interval is present between 2.90 m and 4.75 m. A carbonate-poor interval named Fish Level, corresponding to the sedimentary expression of the T-OAE, consists of dark greenish-grey marly claystone in the lower portion (8.27-10.73 m) and dark brown marly claystone to fissile black shale in the upper part (10.73-12.98 m). The interval above the Fish Level comprises light brownish grey marlstone and limy marlstone organized in 20 to 40 cm-thick strata.

As far as microfacies are concerned, the Domaro Lmst. consist of light brown mudstone-wackestone with pelagic bivalves, radiolarians and echinoderm fragments. The lithostratigraphic boundary between the Domaro Lmst. and Sogno Fm. is marked by an increase of extraclasts (especially quartz and mica). Light brown mudstone passing upward to reddish brown mudstone characterizes the lower portion of the Sogno Fm. Pelagic bivalves, radiolarians and echinoderm fragments are the dominant bioclasts. Just below the Fish Level base, the microfacies consists of light brown wackestone with abundant isoriented pelagic bivalves. Mudstone with high organic matter, clay and dark mineral contents are observed through the Fish Level. Two portions are distinguished on the basis of micrite color and allochem content: the lower part corresponds to dark reddish brown micrite, while the upper part consists of very dark brown micrite with relatively frequent radiolarians, echinoderm fragments and dark minerals. Above

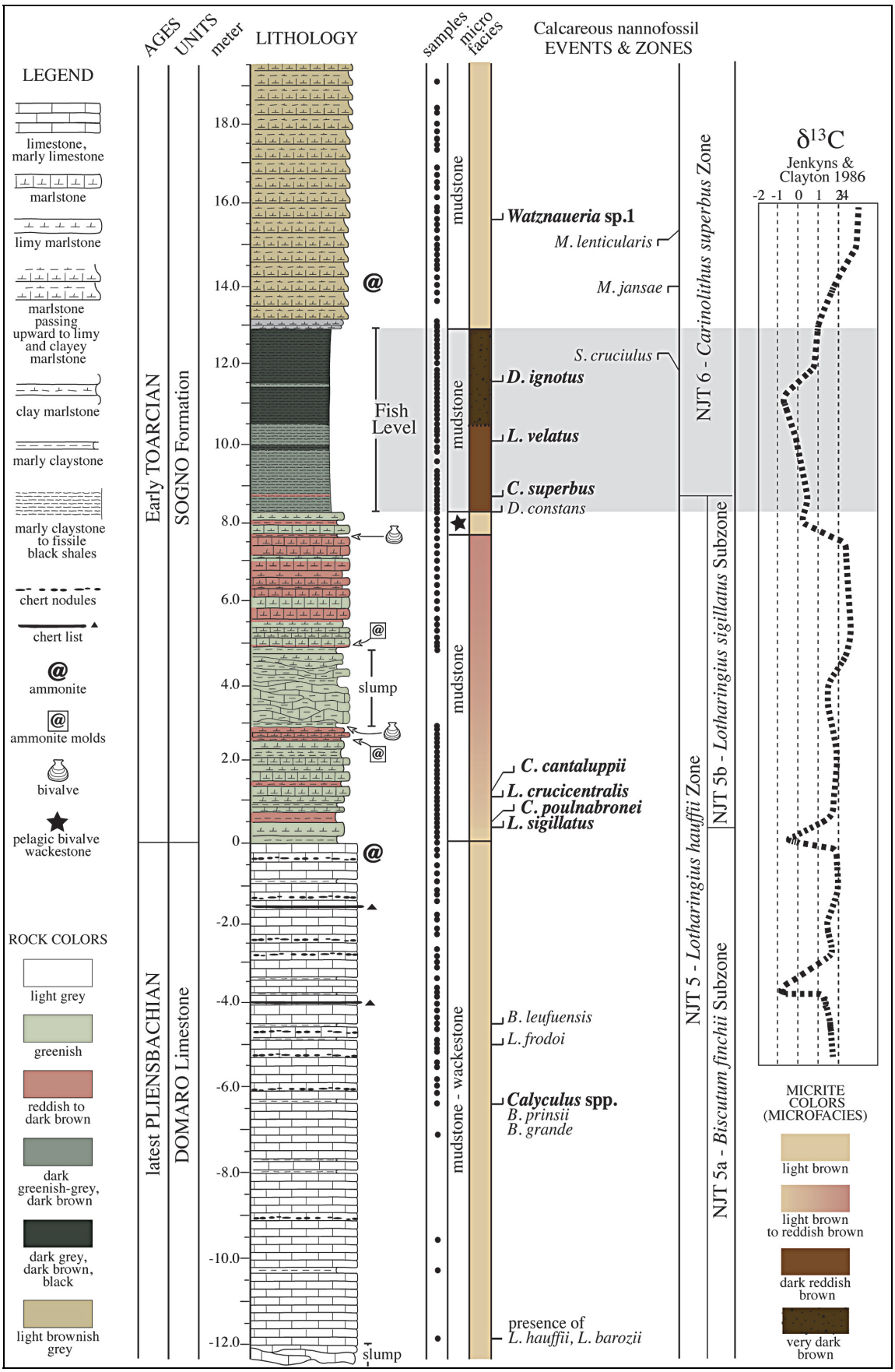

Fig. 3 - Lithostratigraphy and calcareous nannofossil biostratigraphy of the Colle di Sogno section. The main events of Mattioli & Erba (1999) are in bold. @ = ammonite findings after Gaetani & Poliani (1978) are discussed in the text. The C isotope curve is after Jenkyns & Clayton (1986). Microfacies were defined according to Dunham (1962) classification, employing the tables of Baccelle & Bosellini (1965) for percentage estimation of allochems.

the Fish Level mudstone consists of light brown micrite with an allochemical content decreasing upwards.

Materials & Methods

Calcareous nannofossil biostratigraphy was performed on a total of 163 samples (Fig. 3). Average sampling rate is ~20 cm through the section, with exceptions of the lowermost 6 m, having much wider sample spacing, and the interval across the Domaro Lmst./Sogno Fm. boundary and the Fish Level both sampled every 10 cm. Samples were prepared from marly limestones and limestones of the Domaro Lmst. and marlstones, limy marlstones, marly claystones and black shales of the Sogno Fm.

Biostratigraphic analyses were performed on smear slides prepared as follows: a small amount of rock material was powdered adding few drops of bi-distillate water, without centrifuging, ultrasonic cleaning or settling the sediment in order to retain the original composition. The obtained suspension was mounted onto a slide, covered with a cover slide and fixed with Norland Optical Adhesive. Smear slides were investigated using a light polarizing microscope, at 1250X magnification. Calcareous nannofossil preservation and semi-quantitative abundances were evaluated by examining at least 400 fields of view in each smear slide. The biostratigraphic scheme adopted is that of Mattioli & Erba (1999). Calcareous nannofossil taxa recognized are listed in Appendix 1. The range chart is reported in Appendix 2.

Calcareous nannofossil quantitative analyses were performed on 49 samples, selected every 60-80 cm, with exception of the Fish Level analyzed every 40 cm. Absolute abundances were obtained counting all specimens in 1 mm^2 of ultrathin sections (7 μm thick), following the methodology of Erba & Tremolada (2004). For quantitative analyses calcareous nannofossil taxa were counted at the generic level, because the use of ultrathin section partly constrain the identification at specific level. While this type of investigation is ideal for large-sized and highly calcified taxa (e.g. *Mitrolithus, Schizosphaerella)*, that result to be unequivocally detectable and quantifiable, small and medium size coccoliths (e.g. *Biscutum*, *Lotharingius*) are often covered. Moreover, the delicate structure of smaller coccoliths is frequently incomplete due to slicing and thinning of ultrathin sections.

Within genus *Biscutum, B. finchii* is the dominant species while *B. novum*, *B. dubium* and *B. grande* are rare to absent in a few samples. *Lotharingius hauffii* is dominating the *Lotharingius* spp. group, while other species (*L. barozii, L. crucicentralis, L. frodoi*, *L. sigillatus*, *L. umbriensis, L. velatus*) are rare. Concerning *Carinolithus* spp., *C. poulnabronei* and *C. superbus* are equally abundant, while *C. cantaluppii* gives a very little or no contribution. *Crepidolithus crassus* largely dominates the genus *Crepidolithus* since *C. cavus* and *C. granulatus* are sparse. Counting and statistical treatment at generic level were previously adopted by Bour et al. (2007). Also, some datasets of individual species abundances were grouped at generic level for statistical analyses to overcome very low percentages (Tremolada et al. 2006; Aguado et al. 2008; Mattioli et al. 2008; Fraguas et al. 2012; Clémence et al. 2015).

Principal component analysis (PCA) was performed on calcareous nannofossil abundances with the free statistical software Past v1.94b (Hammer et al. 2001). The method to extract factors was eigenvalues. The PCA method facilitates interpretations of complex data sets, reducing large data matrix composed of several variables to a small number of factors representing the main modes of variations (Fukunaga 1990; Beaufort & Heussner 2001). As *Schizosphaerella punctulata* is considered a dinoflagellate cyst (Kälin & Bernoulli 1984), two datasets were used including and excluding this taxon. For both datasets, absolute abundances and percentages (the latter calculated from the total absolute abundances) of all taxa were introduced in the analysis. Furthermore, PCA was performed on both the entire studied interval, and on the interval bounded by the first occurrence (FO) of genus *Carinolithus* and the last occurrence (LO) of *Mitrolithus jansae* in order to consider the real absence or presence within the stratigraphic range of taxa.

Carbonate content analyses were performed on a total of 156 samples. Bulk rock samples were reduced to fine powder in agate mortar. Carbonate content was obtained using a Dietrich–Frühling calcimeter, measuring the CO_2 volume produced by the complete dissolution of pre-weighted samples in 37% vol. HCl. Standards of pure calcium carbonate were measured every five samples to ensure proper calibration.

Microfacies were analyzed on the same 49 thin sections used to achieve calcareous nannofossil absolute abundaces (Fig. 3).

Taxonomic notes

In this paragraph, remarks concerning morphological and/or dimensional features of a few taxa (*B. finchii*, *C. crassus, M. jansae,* and *S. punctulata*) observed under the light polarizing microscope are reported, alphabetically ordered per genus. Furthermore the descriptions of *Rucinolithus* sp. and *Watznaueria* sp. 1 are reported.

Genus *Biscutum* Black *in* Black & Barnes, 1959

Biscutum finchii (Crux, 1984) Bown, 1987

Remarks. In the studied section rare to frequent specimens of *B. finchii* with dimensions smaller than the holotype (5.6 μm length - 4.7 μm width) were observed. The specimens with length < 5.5 μm are here reported as "small *B. finchii* " (Pl. 1, figs. 6-7), while specimens with length = 5.5 μm are reported as *B. finchii* (Pl. 1, figs 8-9) (Appendix 2). The "small *B. finchii*" specimens are characterized by a subcircular outline and prominent distal shield. They partially correspond to the morphotypes named as *B.* aff. *B. finchii* by Cobianchi (1990, 1992) and as "small *B. finchii*" by Picotti & Cobianchi (1996), who separated specimens with length < 6 μm.

Stratigraphic observations. "Small *B. finchii*" is present from the lowermost studied sample, below the FO of *B. finchii*. Similarly, Cobianchi (1992) and Picotti & Cobianchi (1996) documented "small *B. finchii*" in the interval preceding the FO of *B. finchii*, before the FO of *L. hauffii*. In the studied section, *B. finchii* is observed from the uppermost part of the NTJ 5a Subzone, between the FOs of genus *Calyculus* and *L. sigillatus*, at a similar stratigraphic level to that reported by Cobianchi (1992).

Genus *Crepidolithus* Noël, 1965

Crepidolithus crassus (Deflandre *in* Deflandre & Fert, 1954) Noël, 1965

Remarks. The holotype of *Discolithus crassus* has dimensions of 8.2 μm length and 5.5 μm width. Later,

Noël (1965) moved this species in the *Crepidolithus* genus, and pointed out the co-occurrence of specimens with smaller dimensions (3.7-4.4 μm length and 2.3-3.2 μm width). Bown (1987) reported specimens with size ranges of 5.0-9.0 μm for length and 3.5-5.5 μm for width. In this study, specimens displaying length = 5 μm and width = 3.5 μm are attributed to *C. crassus* (Pl. 1, figs 18-19), while specimens with length < 5 μm and width < 3.5 μm are reported as "small *C. crassus*" (Pl. 1, fig. 20) (Appendix 2).

Stratigraphic observations. "Small *C. crassus*" and *C. crassus* co-occur through the studied interval, although the small one presents a discontinuous occurrence and is rarer than the latter.

Genus *Mitrolithus* Deflandre, 1954 *in* Deflandre & Fert, 1954

Mitrolithus jansae (Wiegand, 1984) Bown *in* Young et al., 1986

Remarks. This species was described as *Calcivascularis jansae* by Wiengand (1984), a nannolith of 2.4-5.6 μm length (height) and 3.2-5.6 μm maximum width (holotype: 2.3 μm length – 3.5 μm maximum width). Later, Bown (*in* Young et al. 1986) moved this species in the *Mitrolithus* genus, pointing out a considerable variation in dimensions and reporting a comprehensive size of 4-8 μm, without specify length or width. Bown (1987) also remarked a great size variation, describing ranges of 3.0-4.6 μm for maximum width, and 2.3-5.3 μm for rim height. Later Bown & Cooper (1989) specified a height variability of 2.3-5.6 μm. A notable variation of murolith height was reported by previous Authors (plate 1, Mailliot et al. 2006; plate 1, fig. 5, Fraguas et al. 2008; fig. 5a-c, Bodin et al. 2010; plate 1, figs 9-12, Reggiani et al. 2010b; figs 56-60, Sandoval et al. 2012). Specimens observed in the studied samples show height variability from 3 to 8 μm. Moreover, we noticed that the thickness of outer elements of the murolith varies from 0.5 to 2 μm. Specimens characterized by very thin outer elements (<1 μm) and displaying grey to whitish colours under crossed nicols are distinguished here as "thin *M. jansae*" (Pl. 1, figs 26-27), while specimens with thicker outer elements, displaying bright white to yellow colours, are attributed to *M. jansae* (Pl. 1, fig. 28) (Appendix 2). The structure of the central spine is identical in both morphotypes.

Stratigraphic observations. Specimens of *M. jansae* and "thin *M. jansae*" co-occur in the Domaro Lmst. and in the lower portion of the Sogno Fm. below the Fish Level. "Thin *M. jansae*" is the only morphogroup present through the Fish Level where no regular *M. jansae* specimens were observed. "Thin *M. jansae*" disappears one meter above the top of the black shale interval.

In the studied section, the rim height variability has no stratigraphic significance: tall and short specimens co-occur with comparable abundances through the Domaro Lmst. and the Sogno Fm., displaying similar trends.

Genus *Rucinolithus* Stover, 1966

Rucinolithus sp. ind.

Description. Polycyclolith specimens consisting of 7-9 imbricated elements, with radial symmetry, and showing high birefringence colours. The elements are arranged slightly irregularly and have a petaloid shape with rounded ends. The outline is sub-circular, display-

PLATE 1

Scale bars represent 2 μm.

Figs. 1-2 - *B. dubium*, 1) cross-polarized light, 2) quartz lamina, sample 72B (0.8 m).

Figs. 3-4 - *B. grande*, 3) cross-polarized light, 4) quartz lamina, sample 71A (0.2 m).

Fig. 5 - *B. prinsii*, cross-polarized, sample 71B (0.3 m).

Figs. 6-7 - "small *B. finchii*", 6) cross-polarized light, 7) quartz lamina, sample 84BB (14.5 m).

Figs. 8-9 - *B. finchii*, 8) cross-polarized light, 9) quartz lamina, sample CS-L1-78 (4.80 m).

Fig. 10 - *B. leufuensis*, cross-polarized, sample 73A (1.05 m). 0

Fig. 11-13 - *Calyculus* sp., side view, cross-polarized light, 11) sample 84Z (11.45 m),12) sample 84D (9.45 m), 13) sample 3A (-0.15 m).

Fig. 14-15 - *C. poulnabronei*, side view, cross-polarized light, 14) sample 84P (10.75 m), 15 sample 84U (11.25 m).

Figs. 16-17 - *C. superbus*, 16) cross-polarized light, 17) quartz lamina, sample 84C (9.35 m).

Figs. 18-19 - *C. crassus*, cross-polarized light, 18) sample 3Q (-3.6 m), 19) sample CS-L1-75 (2.6 m).

Fig. 20 - "small *C. crassus*", cross-polarized light, sample TS 38.00 (-9.6 m).

Fig. 21 - *C. cavus*, cross-polarized light, sample 71A (0.2 m).

Fig. 22 - *C. granulatus*, cross-polarized light, sample 71A (0.2 m).

Figs. 23-24 - *D. constans*, 23) cross-polarized, 24) quartz lamina, sample 85B (15.15 m).

Fig. 25 - *M. lenticularis*, cross-polarized, sample 71A (0.2 m).

Figs. 26-27 - "thin *M. jansae*", cross-polarized, 26) sample 73B (1.1 m), 27) sample 3K (-2.3 m).

Fig. 28 - *M. jansae*, cross-polarized, sample 72D (1.0 m).

Figs. 29-30 - *D. ignotus*, 29) cross-polarized, 30) quartz lamina, sample 84AA (11.55 m).

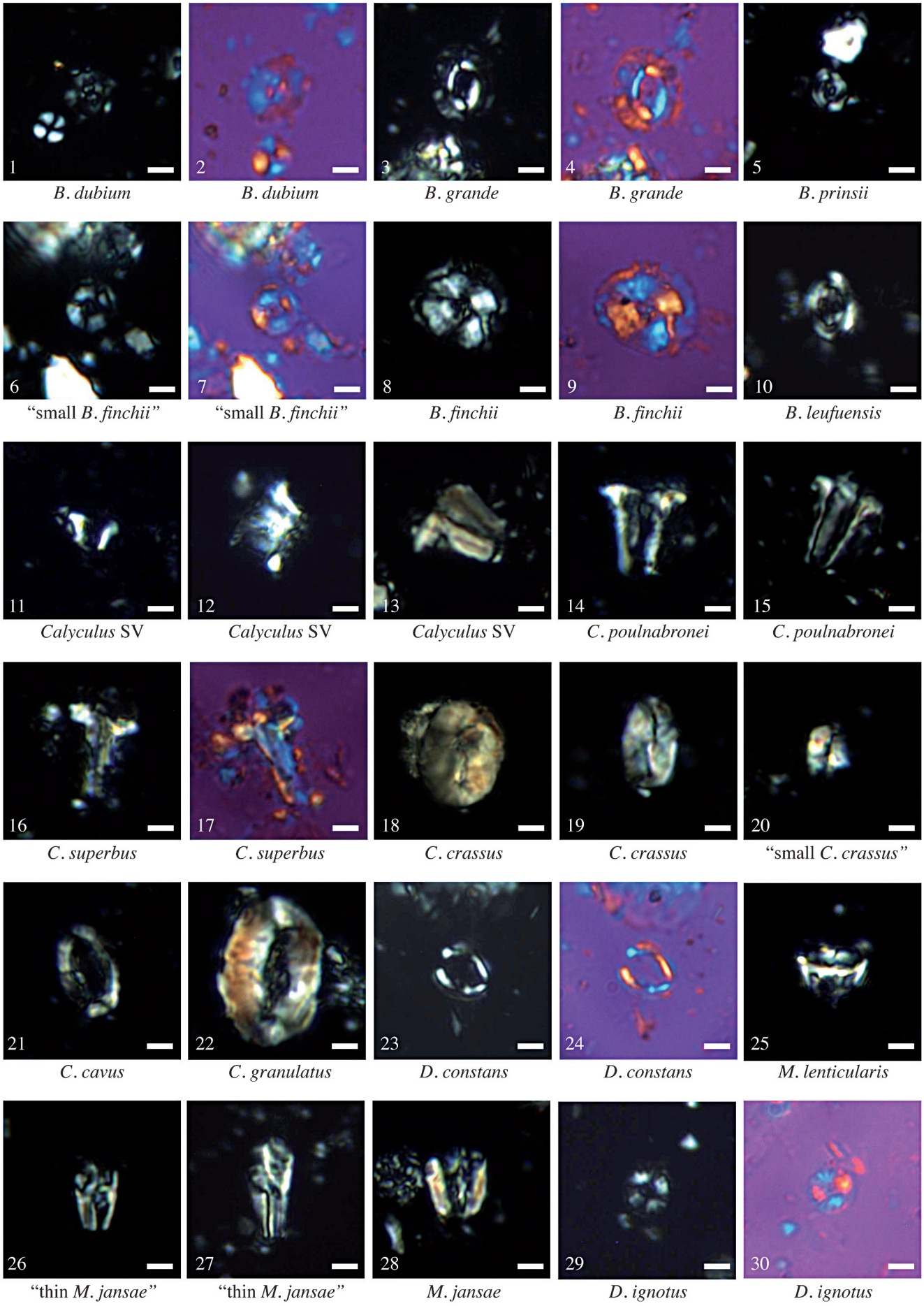

B. dubium *B. dubium* *B. grande* *B. grande* *B. prinsii*

"small *B. finchii*" "small *B. finchii*" *B. finchii* *B. finchii* *B. leufuensis*

Calyculus SV *Calyculus* SV *Calyculus* SV *C. poulnabronei* *C. poulnabronei*

C. superbus *C. superbus* *C. crassus* *C. crassus* "small *C. crassus*"

C. cavus *C. granulatus* *D. constans* *D. constans* *M. lenticularis*

"thin *M. jansae*" "thin *M. jansae*" *M. jansae* *D. ignotus* *D. ignotus*

ing a diameter comprised between 6 and 8 μm (Pl. 2, figs 16-17).

Remarks. The observed specimens are very similar to *R. terebrodentarius* (Covington & Wise 1987; Tremolada & Erba 2002). *Rucinolithus* specimens are common in Cretaceous sequences (Stover 1966; Covington & Wise 1987; Erba 1994, 2004; Burnett 1998; Tremolada & Erba 2002) and were recently described from the Middle Jurassic (Tiraboschi & Erba 2010). This is the first time that *Rucinolithus* is reported from the Lower Jurassic. Specimens observed in this study generally belong to the "small *Rucinolithus*" category of Tiraboschi & Erba (2010, fig. 6 pictures 1-8).

Stratigraphic observations. These nannoliths were observed in the lower part of the studied section up to the base of the Fish Level. They are rare within the NJT 5a Subzone and become extremely rare in the NJT 5b Subzone.

Genus *Schizosphaerella* Deflandre & Dangeard, 1938

Schizosphaerella punctulata
Deflandre & Dangeard, 1938

Remarks. This species was described as a nannolith composed by two interlocked valves with a diameter of 12-30 μm (Deflandre & Dangeard 1938). Later, other Authors pointed out specimens with smaller dimensions: Bown (1987) and Cobianchi (1992) reported a diameter of 8-12 μm, while Mattioli & Pittet (2002) gave a range of 7-13.5 μm. In the studied section specimens displaying dimensions of 4-7 μm are separated as "small *S. punctulata*" (Pl. 2, figs 15, 20) while specimens with diameter = 7 μm are reported as *S. punctulata* (Pl. 2, figs 21-22; Fig. 4A) (Appendix 2). Additionally, specimens surrounded by fringing crust of radiating prismatic crystals were also observed, and grouped as "encrusted *S. punctulata*" (Pl. 2, figs 23-25; Fig. 4B-C-D) (Appendix 2). The thickness of fringes varies from 2 to 5 μm. It is to be pointed out that crusts affect only specimens with a diameter > 7 μm.

Stratigraphic observations. "Small *S. punctulata*" and *S. punctulata* occur together through the studied interval, both showing a drastic decrease in abundance within the Fish Level. "Small *S. punctulata*" is less abundant above the black shale interval. "Encrusted *S. punctulata*" is present in the Domaro Lmst. and in the lower part of the Sogno Fm., prior to the base of the Fish Level.

Discussion. Kälin (1980) described specimens of *S. punctulata* with fringes of radial crystals in samples from the Southern Alps, Tuscany and Umbrian sequences (Kälin 1980, fig. 14), and demonstrated their early diagenetic origin, with formation of neomorphic calcite, possibly controlled by a low Mg/Ca ratio of oceanic waters (Kälin & Bernoulli 1984). Although a diagenetic origin of such crusts is not questioned, we point out that diagenetic processes should affect all *S. punctulata* specimens with a diameter > 7 μm, therefore it is difficult to explain why encrusted morphotype occur together with non-encrusted ones of similar dimensions.

Genus *Watznaueria* Reinhardt, 1964

Watznaueria sp. 1 Cobianchi et al., 1992

Remarks. *Watznaueria* coccoliths 3-5 μm length and 2-4 μm width with a small open central area. At crossed nicols they show white birefringence colours (Pl. 2, figs 18-19).

Discussion. Comparable specimens were reported as *W. aperta* by Erba & Cobianchi (1989). Cobianchi et al. (1992) and Gardin & Manivit (1994) described analogous coccoliths as *Watznaueria* sp. 1, whereas Reale et al. (1992) and Baldanza & Mattioli (1992) reported similar specimens as *W. barnesiae*. Mattioli (1996) revised the latter attribution, ascribing the specimens to *Watznaueria* sp. 1. Mattioli & Erba (1999)

PLATE 2

Scale bars represent 2

Figs. 1-2 - *L. hauffii*, 1) cross-polarized, 2) quartz lamina, sample 5C (-5.0 m).

Figs. 3-4 - *L. frodoi*, 3) cross-polarized, 4) quartz lamina, sample 83A (8.3 m).

Fig. 5, 10 - *L. umbriensis*, cross-polarized, 5) sample 3B (-0.5 m), 10) sample 3B (-0.5 m).

Figs. 6-7 - *L. barozii*, 6) cross-polarized, 7) quartz lamina, sample 71D (0.5 m).

Figs. 8-9 - *L. sigillatus*, 8) cross-polarized, 9) quartz lamina, sample 84R (10.95 m).

Figs. 11-12- *L. crucicentralis*, 11) cross-polarized, 12) quartz lamina, sample 73A (1.05 m).

Figs. 13-14- *L. velatus*, 13) cross-polarized, 14) quartz lamina, sample 84BB (14.5 m).

Fig. 15, 20 - "small *S. punctulata*", cross-polarized, 15) sample 74F (2.4 m), 20) sample 74F (2.4 m).

Figs. 16-17- *Rucinolithus* sp. ind., 16) cross-polarized, 17) quartz lamina, sample 5E (-5.45 m).

Figs. 18-19- *Watznaueria* sp.1, 18) cross-polarized, 19) quartz lamina, sample CS-L1-87 (15.75 m).

Figs. 21-22- *S. punctulata*, 21) cross-polarized, 22) quartz lamina, sample 3C (-0.7 m).

Fig. 23-25 - "encrusted *S. punctulata*", cross-polarized, 23) sample TS 33.80 (-5.12 m), 24) sample 5G (-5.85 m), 25) quartz lamina, sample 5G (-5.85 m).

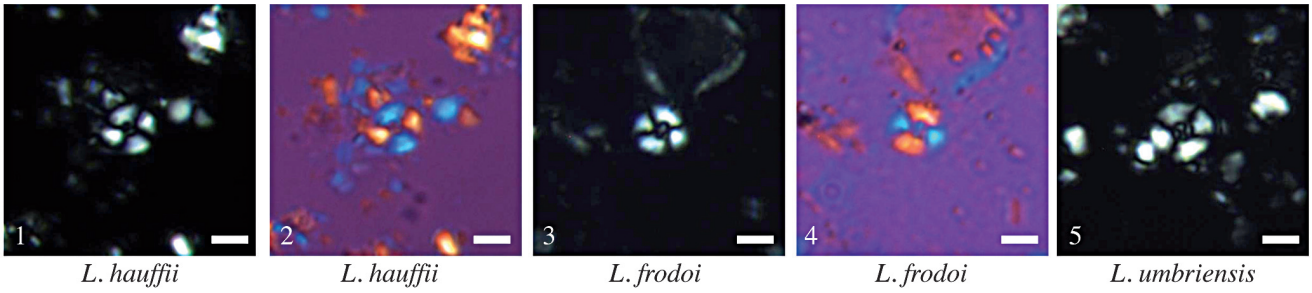

L. hauffii *L. hauffii* *L. frodoi* *L. frodoi* *L. umbriensis*

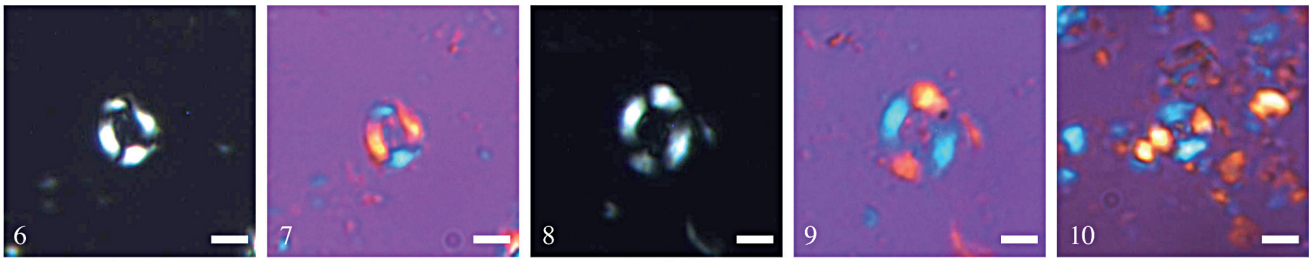

L. barozii *L. barozii* *L. sigillatus* *L. sigillatus* *L. umbriensis*

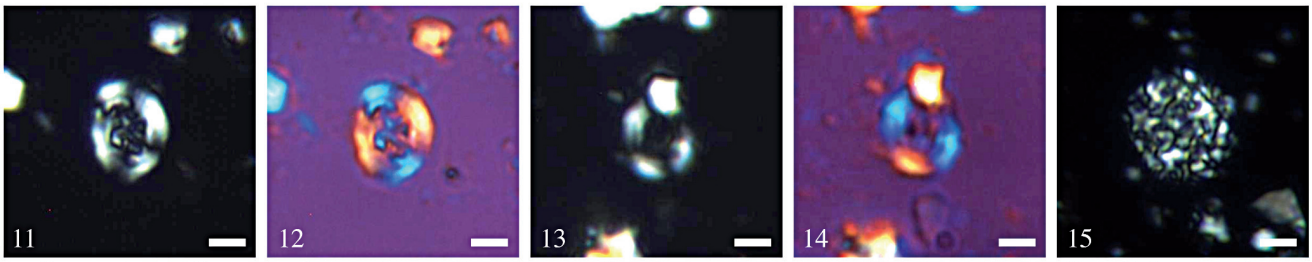

L. crucicentralis *L. crucicentralis* *L. velatus* *L. velatus* "small *S. punctulata*"

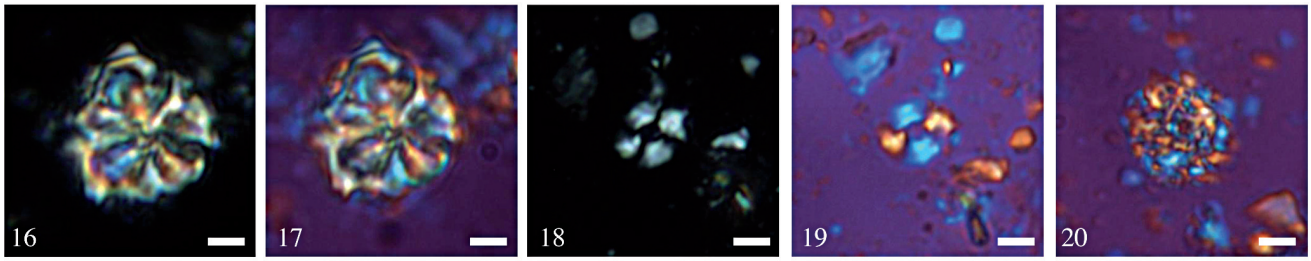

Rucinolithus sp. ind. *Rucinolithus* sp. ind. *Watznaueria* sp.1 *Watznaueria* sp.1 "small *S. punctulata*"

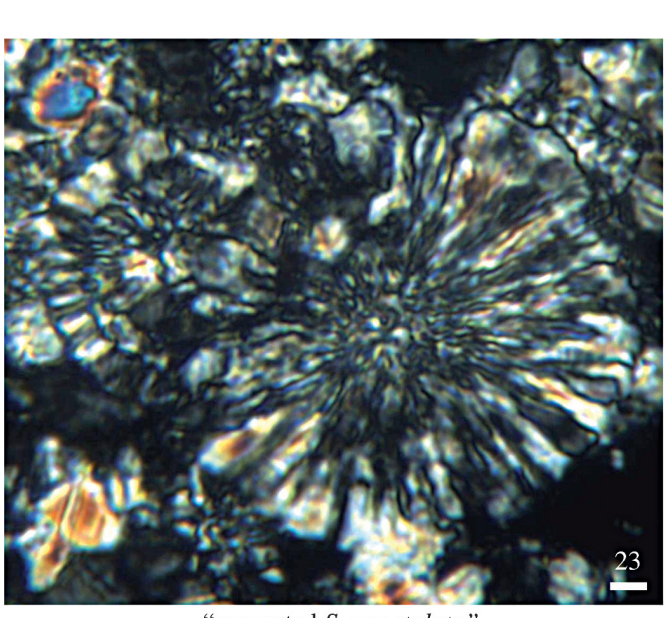

"encrusted *S. punctulata*"

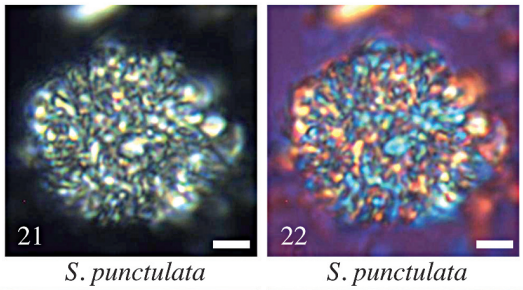

S. punctulata *S. punctulata*

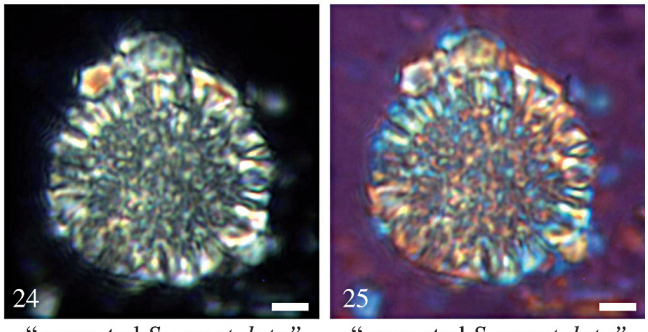

"encrusted *S. punctulata*" "encrusted *S. punctulata*"

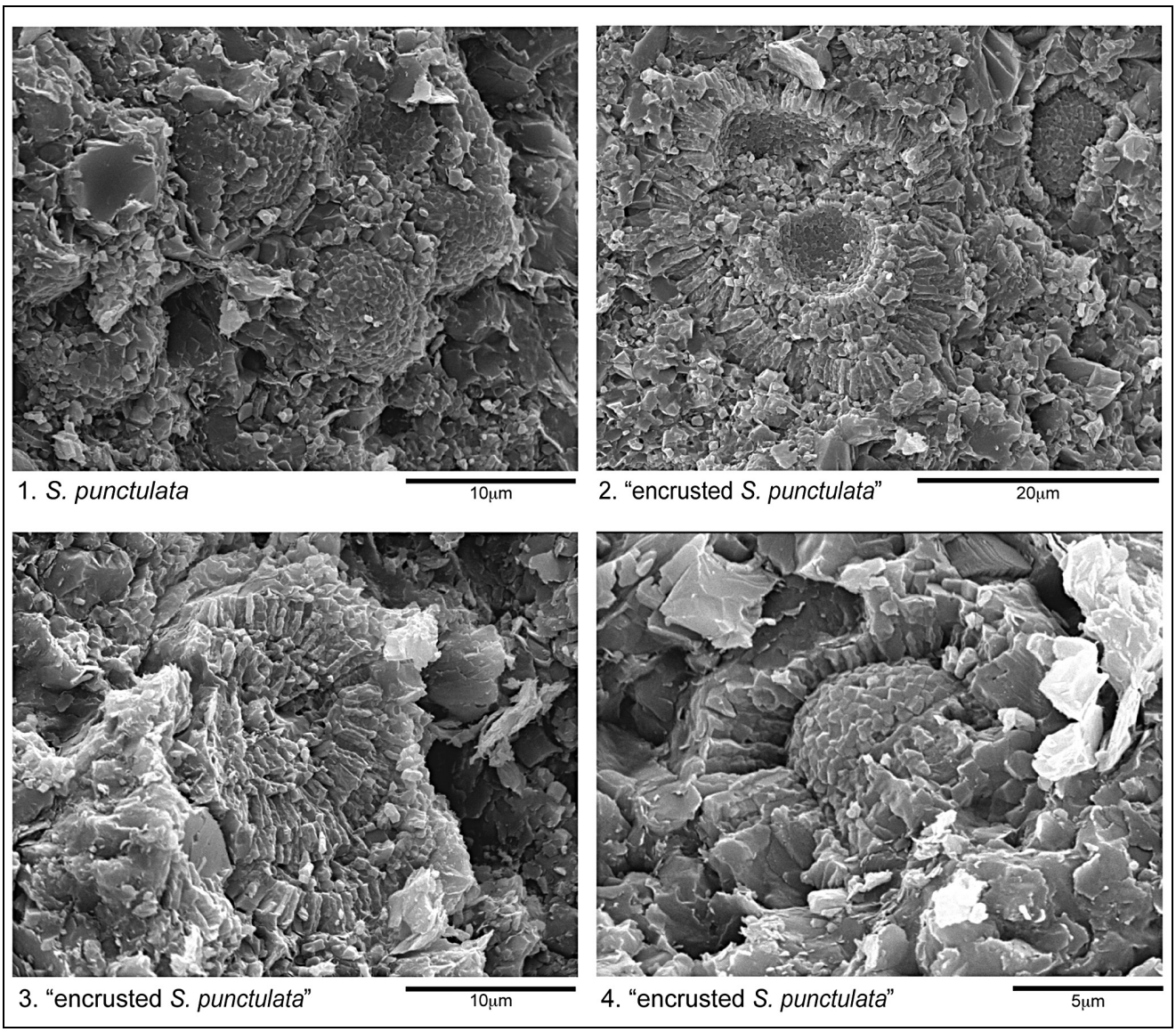

Fig. 4 - 1) *S. punctulata*, sample 79A, 5.65 m; 2) "Encrusted *S. punctulata*", sample 3L, -2.55 m; 3) "Encrusted *S. punctulata*", sample 3D, -0.9 m; 4) "Encrusted *S. punctulata*", sample 79A, 5.65 m. Pictures were taken with the Stereoscan Cambridge 360 scanning electron microscope. Scale bars are quoted on each picture.

used the name *W. fossacincta* for *Watznueria* coccoliths with a small open central area (fig. 10, Mattioli & Erba 1999).

The specimens observed in this study have shield dimensions (both length and width) smaller than *W. fossacincta*, and display a proportionally smaller central opening than *W. fossacincta*. Therefore, we maintain the name *Watznaueria* sp. 1 in analogy with Cobianchi et al. (1992) and Mattioli (1996).

Stratigraphic observations. The FO of *Watznaueria* sp. 1 is the youngest biohorizon detected in the studied section (above the Fish Level) and, as reported by previous Authors (Cobianchi et al. 1992; Mattioli 1996), marks the appearance of genus *Watznaueria* in the Early Toarcian.

Results

Calcareous nannofossil preservation and abundance vary through the studied section, generally increasing from the Domaro Lmst. to the Sogno Fm. Nannofossil preservation seems to be lithology-dependent, improving from limestone to marlstone. Nannofossils from the Domaro Lmst. display a preservation ranging from poor to moderate and a total abundance varying from rare to frequent/common. The marly lithologies of the Sogno Fm. show a slightly better nannofossil preservation (from poor/moderate to moderate) and abundance (frequent/common). In the Fish Level and in the overlying interval abundances fluctuate from rare to common, while preservation is still poor/moderate to moderate. Although the preservation of

calcareous nannofossils ranges from poor to moderate, primary signals are present. In fact, the continuous occurrence of small and delicate taxa, prone to dissolution such as *Biscutum* and delicate species of genus *Lotharingius* (*L. barozii*, *L. velatus*) ensures that diagenesis has not been pervasive. Moreover, these dissolution-prone taxa increase in abundance when robust and dissolution-resistant genera (e.g. *Schizosphaerella* and *Mitrolithus*) show a major decrease that, thus, cannot be ascribed to diagenesis.

Biostratigraphy

The biostratigraphic scheme adopted in this study is that of Mattioli & Erba (1999). Seventeen calcareous nannofossil biohorizons were recognized (Fig. 3), including 9 main and 3 rare biohorizons. Based on the main ones we identified the *Lotharingius hauffii* Zone (NJT 5), divided into *Biscutum finchii* (NJT 5a) and *Lotharingius sigillatus* (NJT 5b) Subzones, and the *Carinolithus superbus* (NJT 6) Zone (Mattioli & Erba 1999).

The oldest investigated sample is assigned to the latest Pliensbachian NJT 5a nannofossil Subzone, based on the presence of *L. hauffii* and *L. barozii* in the lowermost sample (-11.97 m). Within the NJT 5a Subzone few biohorizons were identified: the FOs of *Calyculus*, *B. grande* and *Bussonius prinsii* (-6.4 m), followed by the FOs of *L. frodoi* (-5.0 m) and *Bussonius leufuensis* (-4.55 m). The FO of *L. sigillatus* (0.4 m) defines the NJT 5a/NJT 5b subzonal boundary: this biohorizon approximates in the Tethyan area the Pliensbachian/Toarcian boundary (Mattioli & Erba 1999), that at Colle di Sogno corresponds to the Domaro Lmst./Sogno Fm. lithostratigraphic boundary (Gaetani & Poliani 1978). In the Early Toarcian NJT 5b Subzone, the following biohorizons were detected: FOs of *C. poulnabronei* (0.5 m), *L. crucicentralis* (1.05 m) and *C. cantaluppii* (1.2 m). Near the NJT 5b top, the FO of *Diductius constans* was observed (8.3 m). The FO of *C. superbus* (8.75 m) defines NJT 5/NJT 6 zonal boundary. The top of NJT 6 Zone was not detected due to the absence of *Discorhabdus striatus* in the studied interval. In the NJT 6 Zone, the FOs of *L. velatus* (10.1 m) and *Discorhabdus ignotus* (11.55 m), followed by the LOs of *Similiscutum cruciulus* (11.65 m), *M. jansae* (14.05 m) and *Mitrolithus lenticularis* (15.3 m) were recognized. The youngest biohorizon detected is the appearance of genus *Watznaueria,* with the FO of *Watznaueria* sp.1 (15.6 m).

The calcareous nannofossil assemblage characterizing the NJT 5a Subzone is dominated by *S. punctulata* and *M. jansae* (both frequent to common) and *L. hauffii* (rare/frequent to frequent/common), while genera *Crepidolithus*, *Biscutum* and *Calyculus* are rare. Within *Schizosphaerella, S. punctulata* is dominant (rare/frequent to frequent/common), while "small *S. punctulata*" and "encrusted *S. punctulata*" are subordinated (rare to rare/frequent). Within the *M. jansae* group, "thin *M. jansae*" is dominating (rare/frequent to common), while *M. jansae* is subordinated (rare to rare/frequent).

Assemblage of the NJT 5b Subzone is dominated by *L. hauffii* (frequent to common), *S. punctulata* and *M. jansae* (rare/frequent to frequent/common). Among schizosphaerellids, *S. punctulata* is the dominant form, showing an increase in abundance upwards: in the Sogno Fm. portion below the slumped interval, it is rare to frequent, and becomes frequent to frequent/common between the slumped interval and the Fish Level. "Small *S. punctulata*" is rare to frequent, decreasing upwards. "Encrusted *S. punctulata*" is rare and observed only below the Fish Level. Within the NJT 5b Subzone "thin *M. jansae*" is more abundant (rare/frequent to common) than *M. jansae* (rare to frequent/common); the latter is observed only below the Fish Level. Genera *Carinolithus* and *Biscutum* are rare/frequent to frequent, while genera *Calyculus* and *Crepidolithus* are rare. Through the NJT 5 Zone, extremely rare specimens of *Rucinolithus* sp. were observed.

The taxa dominating the assemblage of NJT 6 Zone belong to the genus *Lotharingius* (*L. hauffii* frequent/common to common/abundant; *L. frodoi* and *L. sigillatus* frequent; *L. velatus, L. crucicentralis* and *L. umbriensis* rare to frequent). The assemblage of the lower part of NJT 6 Zone (corresponding to the Fish Level) is also characterized by genera *Biscutum*, *Calyculus* and *Carinolithus*, which are frequent, while genera *Schizosphaerella, Mithrolithus* and *Crepidolithus* are very rare. The assemblage of the uppermost part of NJT 6 Zone (above the Fish Level) is characterized by rare to frequent *S. punctulata* (both *S. punctulata* and "small *S. punctulata*"), *Biscutum* and *Carinolithus.*

Comparison with previous works

The biohorizons recognized at Colle di Sogno (Fig. 5B) are compared to the events of Mattioli & Erba (1999) to discuss analogies and/or differences. In the latest Pliensbachian-Early Toarcian interval (*spinatum-serpentinus* Ammonite Zones - AZs) Mattioli & Erba (1999) identified twenty-one calcareous nannofossil events (i.e. fourteen main events, five rare and two subjected to further investigations) and defined four zones (Fig. 5A). In the studied section all biohorizons of Mattioli & Erba (1999) were recognized with the exception of FOs of *Similiscutum lowei* and *Watznaueria colacicchii*. The succession of main and rare biohorizons of latest Pliensbachian age at Colle di Sogno shows minor differences with Mattioli & Erba (1999). In fact, the FO of *C. cantaluppii* is detected slightly after the FO of *L. crucicentralis*, most probably due to the rarity of *C. cantaluppii* in the studied material. At Colle di Sogno, the FO of *L. frodoi* is observed after the FO of genus *Calyculus*, possibly because this species is rare in its

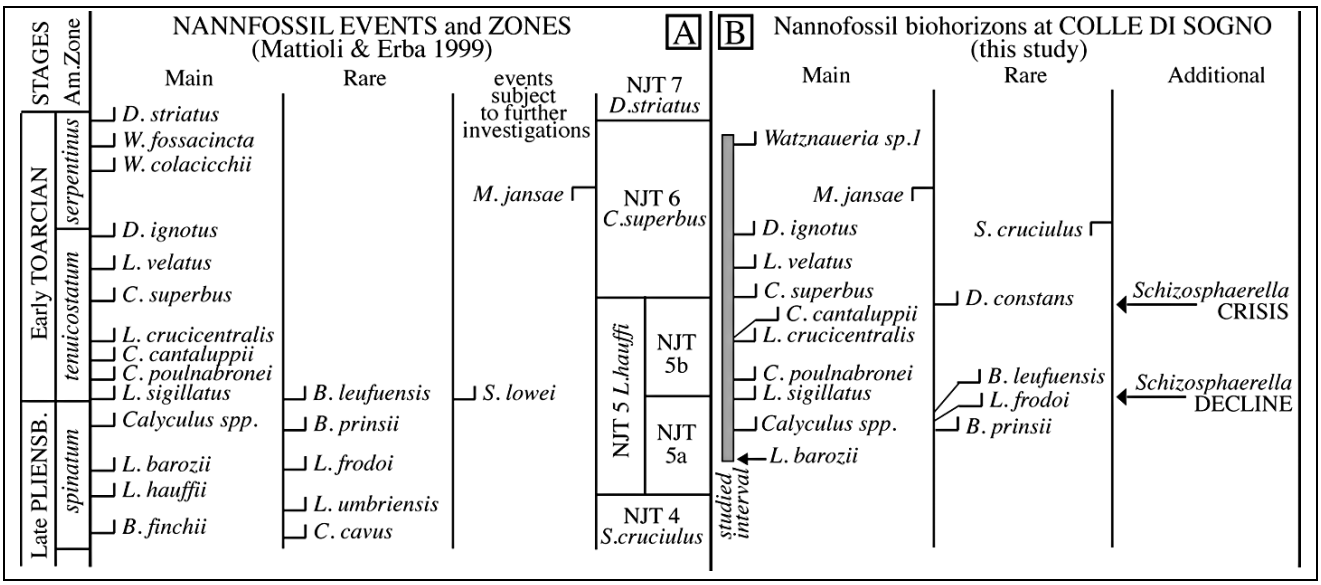

Fig. 5 - Comparison between calcareous nannofossil events detected by Mattioli & Erba (1999) (A) and the biohorizons recognized at Colle di Sogno (B).

lower range. Our results confirm the LO of *M. jansae* (thin specimens) between the FOs of *D. ignotus* and *Watznaueria* sp. 1 (*W. fossacincta* of Mattioli & Erba 1999), thus this biohorizon appears to be reliable and that it can be considered a main one, at least for low-latitude Tethyan sites. The FO of *D. constans*, an event not reported by Mattioli & Erba (1999), was detected below the FO of *C. superbus*, within the NJT 5b Subzone at Colle di Sogno. Gardin & Manivit (1994) reported this biohorizon from the Early Toarcian, below the FO of *Watznaueria* sp. 1; De Kaenel et al. (1996) reported it above the FO of *C. superbus*, while Bown & Cooper (1998) only reported a questionable appearance datum from the earliest Toarcian *tenuicostatum* AZ. Recently, the lowest occurrence of *D. constans* was reported from Southern Spain and Germany, below the FO of *C. superbus* (Mattioli et al. 2004; Sandoval et al. 2012). Our result supports the consistency of the FO of *D. constans* and we put this biohorizon in the group of the rare ones (Fig. 5B). The LO of *S. cruciulus* is observed in the NJT 6 Zone, within the Fish Level. It is bracketed between the FO of *D. ignotus* and the LO of *M. jansae*. Mattioli & Erba (1999) considered this event among the ones subject to further investigations and suggested a LO in latest Aalenian. However, in their literature overview, the LO of *S. cruciulus* is reported in the Early Toarcian (De Kaenel & Bergen 1993; Bown & Cooper 1998). Later this biohorizon was attributed to the Early Toarcian in Greece (Kafousia et al. 2014) and Germany (Mattioli et al. 2004). While Perilli et al. (2004) and Perilli & Duarte (2006) reported this species as discontinuously present until the end of the Toarcian in N Spain and Portugal.

Using the zonation of Mattioli & Erba (1999), in Figure 6 we compare nannofossil biohorizons comprised between the FOs of genera *Calyculus* and *Watznaueria* against ammonite biozones (latest Pliensbachian to Early Toarcian) as documented for sections in Germany, France, Spain, Portugal, Italy and Greece (see Tab. 1 for references). The chronostratigraphy of each calcareous nannofossil event is discussed below in stratigraphic order.

- The FO of *Calyculus* is reported from the middle-upper *emaciatum* AZ in Italy and from the upper *spinatum* AZ in Argentina (Al-Suwaidi et al. 2010). This species is present since the base of the Dotternhausen (Germany) and Sancerre-Couy (France) sections, which are assigned to the upper *spinatum* AZ. In two sections from N Spain (Camino and San Andrés) this genus is reported as rare and discontinuous since the *ibex* and *davoei* AZs, while in one section form Portugal (Peniche) it is present since the *jamesoni* AZ.
- The FO of *L. sigillatus* correlates with the *emaciatum/polymorphum* AZs boundary interval in Portugal, the *emaciatum/tenuicostatum* AZs boundary interval in Italy and lowermost *tenuicostatum* AZ in some Spanish sections. Older first occurrences are reported from N Spanish sections, where this biohorizon falls within the *spinatum* AZ. The FO of *L. sigillatus* correlates with younger levels in Argentina, within the uppermost *tenuicostatum* AZ (Al-Suwaidi et al. 2010). This species is present since the base of the sections in Germany and France, in samples assigned to the upper *spinatum* AZ. The rareness of *L. sigillatus* potentially weakens the reproducibility of its FO, however, Figure 6 evidences, as pointed out by previous Authors (Mattioli & Erba 1999; Mattioli et al. 2013), that this event can be useful to approximate the Plienbachian/Toarcian boundary only at lower latitudes (Italy, Portugal and S Spain), while at higher latitudes this event is older and

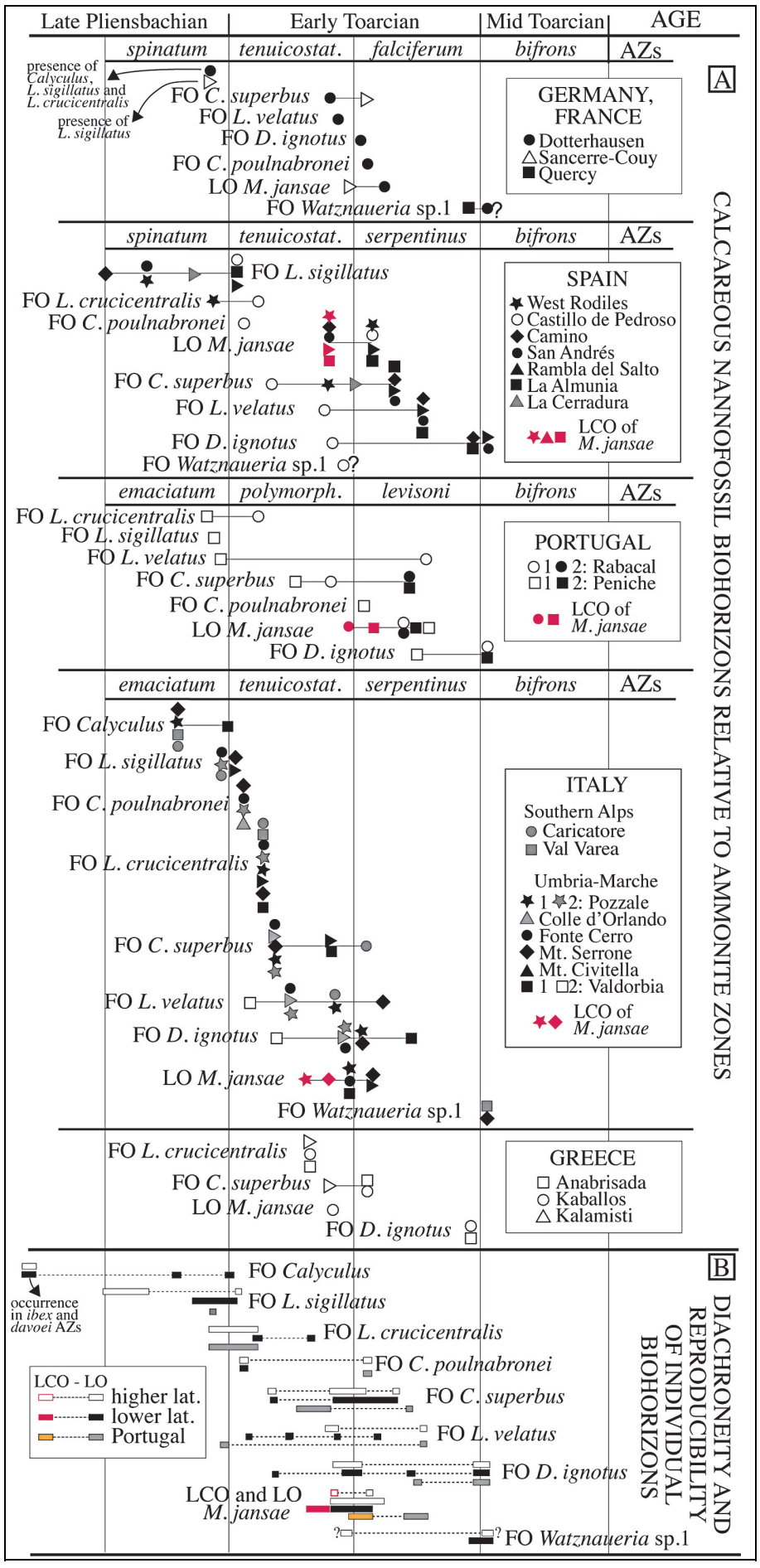

Fig. 6 - A) Main calcareous nannofossil biohorizons plotted against Ammonite Zones from higher and lower latitude sections as synthetized in Tab. 1. Solid symbols identify data derived from published range charts; empty ones refer to works without range charts; B) Diachroneity and reproducibility of individual biohorizons based on ammonite dating.

	COUNTRY	Locality, SECTION NAME (paleoposition, Fig.2)	Ammonite	C isotope	Nannofossils
HIGH LATITUDES	Germany	SW German Basin, DOTTERNHAUSEN (1)	X	X	Mattioli et al. 2004; Bour et al. 2007; Mattioli et al. 2008; Mattioli et al. 2009
	N France	Paris Basin, SANCERRE-COUY drill-core (2)	X	X	Boulila et al. 2014
	N Spain	Basque-Cantabrian Basin, CAMINO (3)	X		Perilli 1999; Perilli & Comas-Rengifo 2002; Perilli et al. 2004; Perilli et al. 2010; Fraguas et al. 2015
		Basque-Cantabrian Basin, SAN ANDRES (3)	X		Perilli 1999; Perilli & Comas-Rengifo 2002; Perilli et al. 2004; Perilli et al. 2010; Fraguas et al. 2015
		Cantabrian Basin, CASTILLO de PEDROSO (3)	X	X	Tremolada et al. 2005
		Asturias, WEST RODILES (3)	X	X	Fraguas & Young 2011; Fraguas et al. 2012; Fraguas et al. 2015
LOW LATITUDES	SW France	Aquitaine Basin, QUERCY (4)	X		Gardin & Manivit 1994
	E Spain	Iberian Range, RAMBLA DEL SALTO (5)	X		Perilli 2000
	E Spain	Iberian Range, LA ALMUNIA (5)	X		Perilli 2000
	S Spain	South Iberian, LA CERRADURA (6)	X	X	Sandoval et al. 2012; Reolid et al. 2014
	Portugal	Lusitanian Basin, RABACAL (7)	X		(1) Baldanza & Mattioli 1992; (2) Perilli & Duarte 2006
		Lusitanian Basin, PENICHE (7)	X	X	(1) Baldanza & Mattioli 1992; Mattioli et al. 2008; Reggiani et al. 2010a,b; Mattioli et al. 2013 (2) Perilli & Duarte 2006;
	N Italy	Lombardy Basin, COLLE DI SOGNO (* - 8)	X	X	Erba 2004; Channell et al. 2010; *this study*
		Lombardy Basin, CARICATORE (8)	X		Cobianchi 1990; Cobianchi 1992
		Lombardy Basin, VAL VAREA (8)	X		Cobianchi 1992
	Central Italy	Umbria-Marche, VALDORBIA (9)	X	X	(1) Reale 1989; Reale et al. 1992 (2) Mattioli et al. 2013
		Umbria-Marche, MONTE SERRONE (9)	X		Reale et al. 1992; Bucefalo Palliani & Mattioli 1998
		Umbria-Marche, MONTE CIVITELLA (9)	X		Reale et al. 1992
		Umbria-Marche, POZZALE (9)	X	X	(1) Reale et al. 1992 (2) Bucefalo Palliani & Mattioli 1998; Mattioli & Pittet 2004; Mattioli et al. 2004
		Umbria-Marche, SOMMA (9)		X	Bucefalo Palliani & Mattioli 1998; Mattioli & Pittet 2002; Mattioli et al. 2004
		Umbria-Marche, COLLE D'ORLANDO (9)	X		Bucefalo Palliani & Mattioli 1998; Mattioli & Pittet 2004
		Umbria-Marche, FONTE CERRO (9)	X		Bucefalo Palliani & Mattioli 1998; Mattioli & Pittet 2004
	NW Greece	Lefkas Island, ANABRISADA, KABALLOS, KALAMISTI (10)	X		Baldanza & Mattioli 1992
		Epirus region, TOKA (10)		X	Kafousia et al. 2014

Tab. 1 - Sections considered in Figs 6 and 7. For each section the papers describing calcareous nannofossil distribution are reported. The presence of ammonite zones and/or chemostratigraphy is also included. Number after each section name corresponds to the paleogeographic position reported in Fig. 2.

dated as latest Pliensbachian (Bown et al. 1988; Fraguas et al. 2015).

• The FO of *L. crucicentralis* is reported from the *tenuicostatum* AZ, although at different levels, in Italy and Greece. An older occurrence is reported from Germany, Spain and Portugal where it correlates with the uppermost *spinatum*-lowermost *tenuicostatum* AZs, or with the uppermost *emaciatum*-lowermost *polymorphum* AZs.

• The FO of *C. poulnabronei* is reported from the lower *tenuicostatum* AZ in Spain and Italy, whereas in Germany and Portugal this taxon has a younger FO in the lowermost *falciferum* and *levisoni* AZs, respectively.

• The FO of *C. superbus* is reported from the lower-middle *tenuicostatum* and middle *polymorphum* AZs to the lower-middle *falciferum, serpentinus* and *levisoni* AZs. While in most Italian sections the FO of *C. superbus* is dated as lower-middle *tenuicostatum* AZ, in most Spanish and Portugal sections it correlates with the middle *serpentinus* and middle *levisoni* AZs, respectively.

• The FO of *L. velatus* is reported from the lower *tenuicostatum* AZ to the middle *serpentinus* AZ in Germany, Spain and Italy. This biohorizon correlates with two different levels in Portugal: uppermost *emaciatum* AZ and middle *levisoni* AZ.

• The FO of *D. ignotus* is reported from Italy and one Spanish section (Castillo de Pedroso) in the interval across the *tenuicostatum/serpentinus* AZs boundary, while in Germany is from the base of the *falciferum* AZ. In the other Spanish sections and in Greece, this biohorizon correlates

with the interval across the *serpentinus/bifrons* AZs boundary. In Portugal it is reported from the middle *levisoni* to the base of *bifrons* AZs.

• The LO of *M. jansae* ranges from the uppermost *tenuicostatum* to the lower *falciferum* and lower *serpentinus* AZs in Germany, France, Spain, Italy and Greece. In Portugal this biohorizon is younger, as it is reported from the middle *levisoni* AZ. In most sections from Spain (La Almunia, Rambla del Salto), Portugal (Rabacal, Peniche) and Italy (Pozzale, M.te Serrone) and in one section from higher latitudes (West Rodiles, N Spain) it is possible to separate the "last common occurrence" (LCO) from the LO of *M. jansae* based on its abundance and range continuity (Fig. 6). At lower latitudes, the LCO of *M. jansae* correlates with the middle-upper *tenuicostatum* AZ (Italy and Spain), while in Portugal this biohorizon correlates with the *polymorphum/levisoni* AZ boundary interval. At higher latitudes, in the West Rodiles section, the LCO corresponds to the upper *tenuicostatum* AZ.

• The FO of *Watznaueria* sp. 1 was documented with certainty only from France and Italy, where it correlates with the top of *falciferum* and the base of the *bifrons* AZs, respectively. It might be that the FO of *W. fossacincta* reported from Germany and Spain corresponds to the FO of *Watznaueria* sp. 1 (see taxonomic notes); if so, then the event is dated as latest *tenuicostatum* and earliest *bifrons* AZs in Spain and Germany, respectively.

The critical evaluation of nannofossil biohorizons calibrated to ammonite zones (Fig. 6B) evidences that the succession of nannofossil events is consistent with the scheme of Mattioli & Erba (1999) and reproducible, with the only exception of older FOs of *L. velatus* when the revisions of the Valdorbia and Peniche sections (Mattioli et al. 2013) are taken into account. Nevertheless, time discrepancy of various extents is derived for all nannofossil biohorizons. In some cases diachroneity seems justifiable by the rareness of taxa, especially in their initial ranges, and in part with very poor preservation of nannofossil assemblages (e.g. Greek sections, Baldanza & Mattioli 1992); the delicate structures of some species (e.g. *L. velatus*) and taxonomic uncertainties (e.g. *W. fossacincta* versus *Watznaueria* sp. 1) may also contribute to the documented diachroneity. Even if the available dataset is limited, latitudinal time-differences of some biohorizons are recognized. This is the case for the FOs of *L. sigillatus* and *L. crucicentralis*, which are older at higher latitudes, while the FO of *L. velatus* is older at lower latitudes (Fig. 6B). Data from Portugal are different relative to both higher and lower latitudes and no systematic patterns are recognizable. For *M. jansae*, both the LCO and the LO appear to be coeval at lower and higher latitudes. However, in Portugal both biohorizons are younger. Figure 6 suggests that the generalized diachroneity of nannofossil events could also result from the calibration to ammonite biozones, known to be controlled regionally (Jenkyns et al. 2002). Mattioli & Erba (1999) demonstrated that their Tethyan nannofossil scheme is largely correlatable with the Boreal one (Bown et al. 1988; Bown & Cooper 1998) (Mattioli & Erba 1999, fig. 12), overcoming the paleoprovincialism shown by ammonites (Elmi et al. 1993).

As suggested by Hesselbo et al. (2007), chemostratigraphy is probably a best framework to test the synchroneity of biohorizons and, consequently, in Fig. 7 we consider nannofossil events against the C isotopic anomaly associated to the T-OAE for sections where these datasets are available (Tab. 1), expanding the previous calibration of the FOs of *C. superbus* and *D. striatus* done by Mattioli et al. (2004). Since the C isotope curves available for most of the considered sections have low resolution, we used a generalized curve following Hesselbo et al. (2007, fig. 1) and subdivided the analysed interval in five sub-intervals: pre-anomaly (sub-interval a), rapid decrease (sub-interval b), minimum (sub-interval c), recovery (sub-interval d) and post-anomaly (sub-interval e) phases. Individual calcareous nannofossil events are discussed below in stratigraphic order.

• The FO of *L. velatus* show diachroneity among different sections: in Italy this biohorizons correlates with C isotopic sub-intervals a to e, while it was found in sub-interval a in sections from Portugal, N Spain and Germany.

• The FO of *D. ignotus* is correlatable to C isotoptic sub-intervals a to e in Italian sections, while this biohorizon correlates with sub-intervals a and d in Portugal and Greece, respectively. In sections from N Spain and Germany the FO of *D. ignotus* falls within C isotopic sub-interval b.

• The FO of *C. poulnabronei* correlates with isotopic sub-interval a in Italy and N Spain, with sub-interval b in Portugal, and with sub-interval c in Germany.

• The FO of *C. superbus* correlates with C isotopic sub-interval a in Portugal and Germany, with sub-intervals a to b in N Spain and Italy, while this biohorizon falls within sub-interval b in S Spain and within sub-interval c in France.

• The LO of *M. jansae* correlates with sub-intervals b, c and d in France, Germany and Portugal, respectively. In sections fron Italy and N Spain this biohorizion spans sub-intervals d and e. When the LCO of *M. jansae* is considered, it correlates with sub-intervals a and c in Italy, a in N Spain and c in Portugal. This datum is not distinguishable in sections from France, Germany, S Spain and Greece.

• The FO of *D. striatus* is correlatable to C isotopic sub-interval e in all analysed sections.

• The FO of *Watznaueria* sp. 1 is correlatable with C isotopic sub-interval e at Colle di Sogno, while

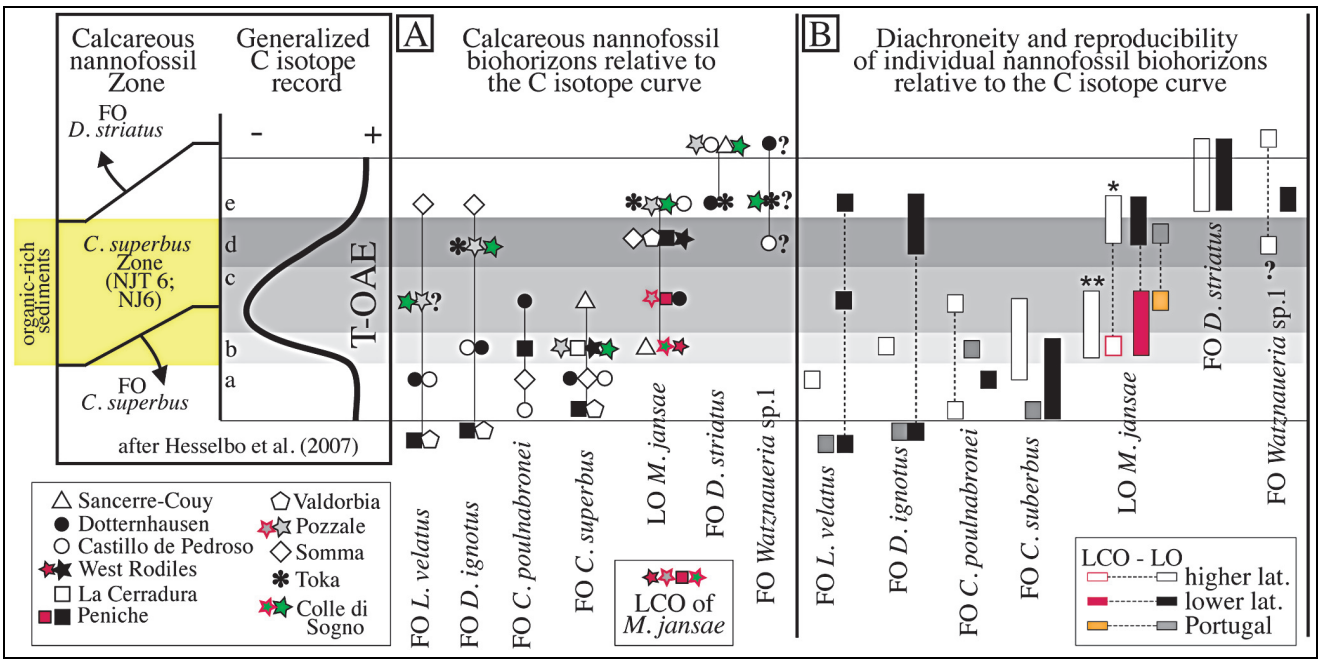

Fig. 7 - A) Selected calcareous nannfossil biohorizons plotted against the C isotope generalized curve, divided into five intervals as follows: a) pre-excursion, white band; b) rapid decrease, light grey band; c) interval with minimum values, medium gray band; d) recovery, dark grey band; e) values comparable to the pre-excursion ones, white band. Following Hesselbo et al. (2007), the yellow box indicates organic-rich sediments deposited during the T-OAE. B) Diachroneity and reproducibility of individual biohorizons relative to the C isotopic anomaly. The FO of *D. striatus* at Colle di Sogno is reported after Erba (2004). See Tab.1 for bibliographic details regarding data reported.

this biohorizon was not unequivocally documented in sections with C isotopic chemostratigraphy. However, if the FO of *W. fossacincta* reported from Germany, N Spain and Greece corresponds to the FO of *Watznaueria* sp. 1 (see taxonomic notes) then this event spans the C isotopic sub-intervals d to e.

The evaluation of nannofossil biohorizons calibrated against the C isotope generalized curve (Fig. 7B) evidences some differences in the sequence of events relative to the one reported in Figure 6B and the scheme of Mattioli & Erba (1999). We notice that the only discrepancies derive from recent re-examitation of the Valdorbia and Peniche sections (Mattioli et al. 2013) that resulted in older FOs of *L. velatus* and *D. ignotus* (Fig. 6B).

When the C isotopic anomaly is taken as reference, the nannofossil biohorizons show some diachroneity, although much reduced relative to the calibration against ammonite zones. This reinforces the problematic use of ammonite zonation as stratigraphic framework (Jenkyns et al. 2002; Mattioli et al. 2004; Hesselbo et al. 2007). Possible reasons for some of the diachronous events might reside in rareness of a few species, especially in their early range (e.g. *L. velatus* and *D. ignotus*) and taxonomic uncertainties (e.g. *W. fossacincta* versus *Watznaueria* sp. 1). In Figure 7B, latitudinal time-differences of some biohorizons are recognized: in fact, *C. poulnabronei* first appears at higher latitudes, while the FO of *C. superbus* is older at lower latitudes. When the C isotopic curve is taken as reference, the dataset from Portugal is consistent with lower latitude records.

In sections from France and Germany, it is not possible to separate the LCO from the LO of *M. jansae*: here the LO of this taxon is older than in the other areas. In most sections from N Spain, Portugal and Italy, instead, the LCO of *M. jansae* is distinguished from its LO (Fig. 7). We underline that the LCO of *M. jansae* at lower latitudes correlates with the LO at higher latitudes (Fig. 7B). Indeed, the record from N Spain (West Rodiles section) shows that *M. jansae* experienced first a LCO at stratigraphic levels comparable to the LCO at lower latitude and LO at higher latitudes, and later a LO coeval with the LO at lower latitudes. The LCO of *M. jansae* is evidenced by the drop in abundance of *M. jansae* and the disappearance level of the normal morphotypes, as documented in this study (Fig. 8).

Our results, complementing previous data, show that few nannofossil events constrain the T-OAE C isotopic anomaly and are traceable among different regions. Specifically, although *C. superbus* is discontinuous at higher latitudes, its FO correlates with the onset of T-OAE at supraregional scale, as also pointed out by Mattioli et al. (2004) and illustrated by Hesselbo et al. (2007). Our analyses confirm that the FO of *D. striatus* is useful to approximate the end of the T-OAE C isotopic anomaly (Mattioli et al. 2004; Hesselbo et al. 2007). The critical evaluation of *M. jansae*

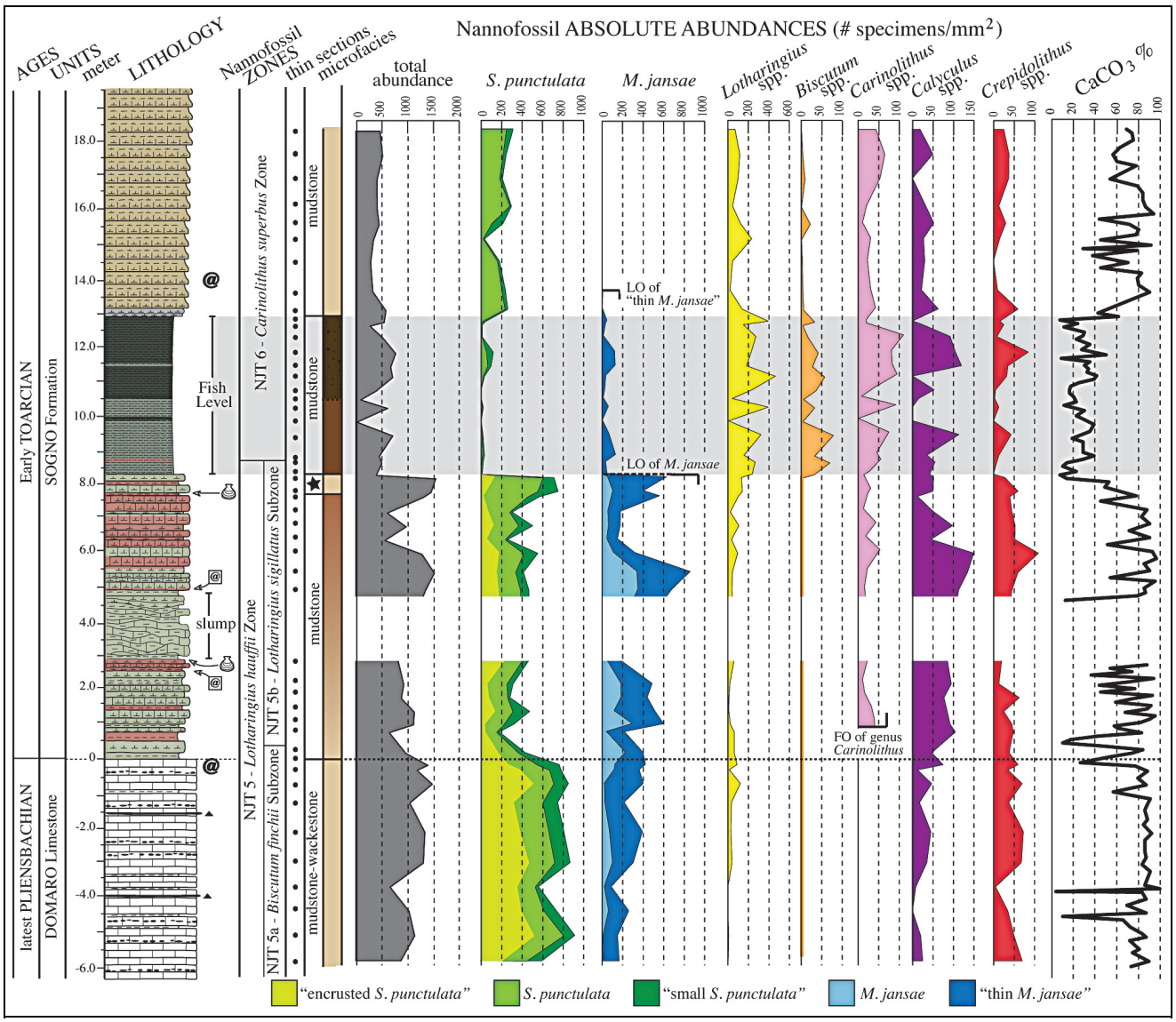

Fig. 8 - Calcareous nannofossil absolute abundances and carbonate content (% $CaCO_3$) of the Colle di Sogno section. For lithology and microfacies legend see Fig. 3.

disappearance level allowed the separation of its LCO preceding the LO. These biohorizons are more evident at lower latitudes, where *M. jansae* is a common component of Pliensbachian-lowermost Toarcian assemblages and shows a marked decrease in abundance in the early phase of the C isotopic anomaly (sub-intervals b and c). At similar stratigraphic levels, the LO of *M. jansae* is reported at higher latitudes. Taking into account latitudinal differences, the LO of *M. jansae* is here proposed as additional event to approximate the end of the T-OAE at lower latitudes, where the LCO is very close to the FO of *C. superbus*. The record from N Spain (West Rodiles section documented by Fraguas et al. 2015) suggests that the LCO and LO can be separated also at relatively higher latitudes where both events are coeval with those documented at lower latitudes.

Absolute abundances

The quantitative investigation of ultrathin sections revealed that the nannofossils total abundance is highest in the Domaro Lmst. and the lower part of the Sogno Fm. (~1000 specimens/mm^2), without significant changes at the sharp lithostratigraphic boundary between the two formations (Fig. 8). At the base of the Fish Level total abundance is halved remaining at similar values across the black shales and overlying interval (Fig. 8).

The carbonate content mostly trace the fluctuations in nannofossil absolute abundances, with the exception of the interval above the Fish Level where $CaCO_3$ values of ~60-80 % correlate with low abundances around 500 specimens/mm^2. The *S. punctulata* and *M. jansae* morphogroups constitute most of the micrite through the Domaro Lmst. and Sogno Fm. below the Fish Level. In the black shale interval both *S.*

punctulata and *M. jansae* drop in abundance while an increase in abundance is observed for small coccoliths that, however, do not contribute much to calcite, justifying the low carbonate content. In the interval above the Fish Level, nannofossils are mostly represented by small taxa with some contribution by *S. punctulata*; this is possibly the reason for a relatively high $CaCO_3$ content. As previously discussed for other intervals (Erba & Tremolada 2004), it is clear that the number of specimens *per se* does not reflect the amount of biogenic calcite since the volume-mass of individual taxa play a crucial role for micrite production.

Total *S. punctulata* abundance (*S. punctulata* + "small *S. punctulata*" + "encrusted *S. punctulata*") shows the highest values within the Domaro Lmst. (~750 specimens/mm^2). In the Sogno Fm., after an initial decrease to a minimum of ~170 specimens/mm^2, the *S. punctulata* mean abundance fluctuates around ~400 specimens/mm^2 up to 7.5 m. The interval below the base of the Fish Level displays an increase up to ~750 specimens/mm^2. Across the Fish Level the abundance of *S. punctulata* drop to 0-100 specimens/mm^2. In the interval above the Fish Level a slight recovery is underlined by an increase of *S. punctulata* to ~230 specimens/mm^2. Within the *S. punctulata* group, "encrusted *S. punctulata*" is dominating in the Domaro Lmst. (~370 specimens/mm^2), drops in abundance across the Domaro Lmst./Sogno Fm. boundary (~90 specimens/mm^2), and is not observed in the Fish Level and the overlying interval. "Small *S. punctulata*" shows a slight decrease in abundance from the Domaro Lmst. (~130 specimens/mm^2) to the Sogno Fm. (~75 specimens/mm^2), and further decreases to a mean of ~10 specimens/mm^2 in the Fish Level. In the overlying interval, abundance partially recovers to ~25 specimens/mm^2. The abundance of *S. punctulata* remains relatively constant (a mean of ~250 specimens/mm^2) from the base of the section to 7.5 m, where this taxon increases up to ~500 specimens/mm^2, with an abundance peak preceding the Fish Level. In the black shale interval *S. punctulata* sharply falls to values lower than 50 specimens/mm^2. A recovery to abundances of ~200 specimens/mm^2 is recorded in the interval above the Fish Level.

The changes in abundance of genus *Schizosphaerella* are similar to those observed in previous studies performed using different methodologies (simple smear slides, settling slides, thin sections). The "*Schizosphaerella* decline" was recognized and defined by Tremolada et al. (2005, fig. 2) on the basis of a marked reduction of *S. punctulata* relative abundance (%). Similar trends are recognizable in Portugal as a drop of *S. punctulata* and total nannofossil abundances (number of nannofossils per grams of rock) (Mattioli et al. 2008, fig. 2c) and *S. punctulata* size (Mattioli et al. 2004, fig. 2; Suan et al. 2008, fig. 2). The "*Schizosphaerella* crisis" was defined in the earliest Toarcian as the drop in abundance of *S. punctulata* just prior the T-OAE black shale determining the end of the dominance of this rock-forming taxon (Erba 2004, figs. 8-9; Tremolada et al. 2005, figs. 2-3). Similarly, a decrease of *S. punctulata* and nannofossil absolute abundances (number of nannofossils per gram of rock) (Mattioli et al. 2008, fig. 2c) as well as *S. punctulata* size (Suan et al. 2008, fig. 2) is recognizable in Portugal just below the C isotope negative excursion. In Spain the "*Schizosphaerella* crisis" could be identified within a decrease in *S. punctulata* and nannofossil absolute abundances (number of nannofossils per gram of rock) (Fraguas et al. 2012, fig. 2) and the minimum of *S. punctulata* and *M. jansae* relative abundances (%), both coinciding with the highest TOC values and the base of the C isotope negative excursion (Fraguas et al. 2012, fig. 3). Hermoso et al. (2012, fig. 3) analysed at ultra high-resolution the behaviour of calcareous nannofossils across the base of T-OAE in the Sancerre-Couy drill core (France), and found a marked decline of *S. punctulata* and coccoliths absolute abundances (number of specimens per gram of sediments) just prior the onset of the negative C isotope excursion and the onset of black shale deposition.

Data gained at Colle di Sogno (both absolute and semi-quantitative abundances) permit to identify the "*Schizosphaerella* decline", correlating with the Domaro Lmst./Sogno Fm. boundary, and corresponding to the Pliensbachian/Toarcian boundary. Furthermore, the "*Schizosphaerella* crisis" is spectacularly well expressed at Colle di Sogno, where at the base of the Fish Level (corresponding to the onset of the T-OAE) *S. punctulata* abundances dramatically drop, accompanied by a contemporaneous major decrease of *M. jansae* and paralleled by an increase of placolith genera, as highlighted by Tremolada et al. (2005). Considering these data, it is evident that the "*Schizosphaerella* decline" and the "*Schizosphaerella* crisis" are biohorizons traceable at supraregional scale and they are here used and proposed as additional biohorizons (Fig. 5B) to approximate the Pliensbachian/Toarcian boundary and the T-OAE onset, respectively.

Contrary to *S. punctulata*, the abundance of the *M. jansae* group shows an increase across the Pliensbachian/Toarcian boundary: in the Domaro Lmst. the total abundance varies from values of 165 specimens/mm^2 (at the base) to 420 specimens/mm^2 (at the top), and "thin *M. jansae*" is dominating over *M. jansae*. A further increase to ~850 specimens/mm^2 is observed in the Sogno Fm. up to 5.5 m: in this interval *M. jansae* displays a marked increase in abundance while the thin morphotypes remain rather constant. A decrease to ~150 specimens/mm^2 due to a major drop of both thin and normal *M. jansae* nannoliths precedes an abundance peak of "thin *M. jansae*" of 580 specimens/mm^2 just below the Fish Level. Notably, only "thin *M. jansae*" specimens are observed in the black shale interval,

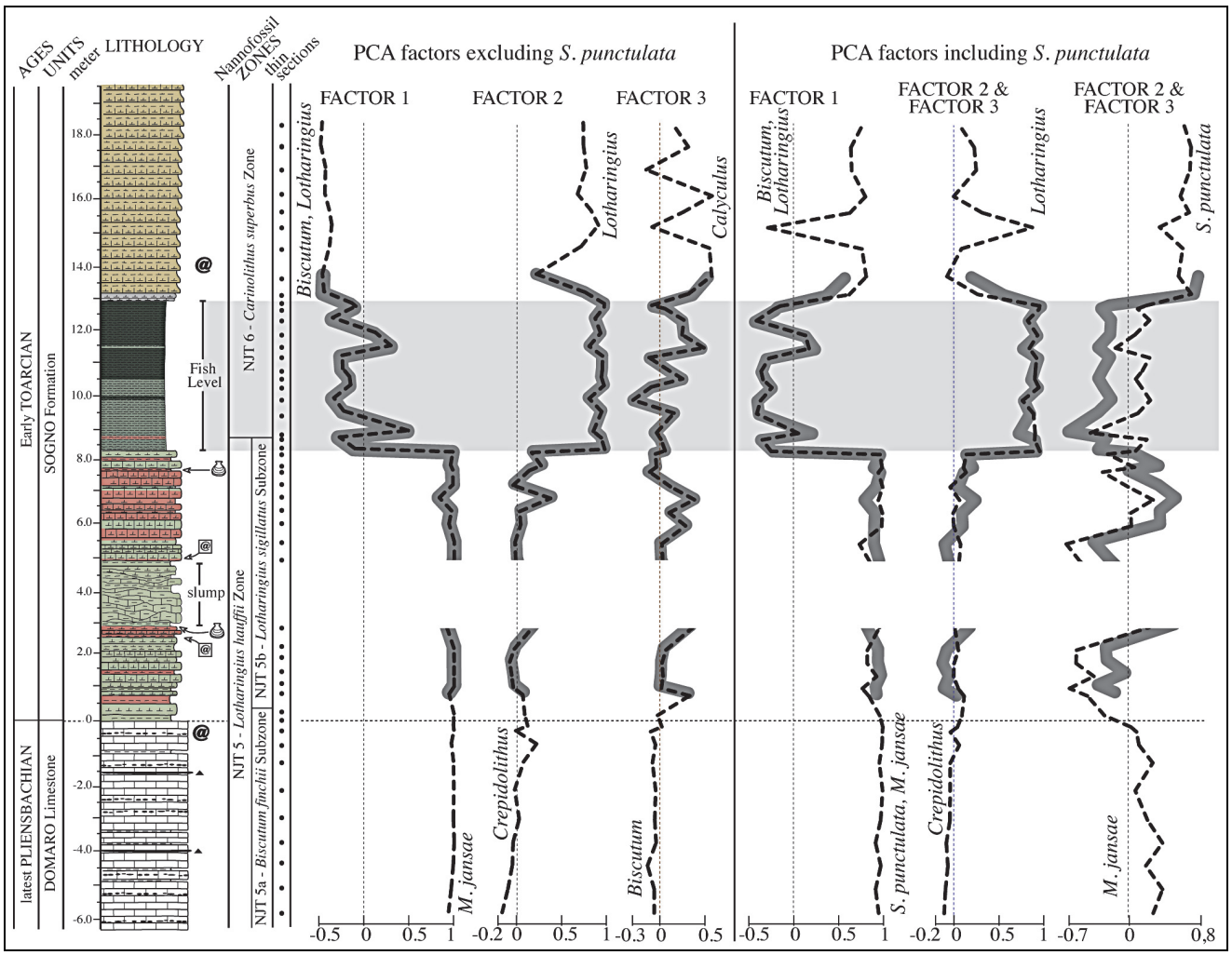

Fig. 9 - Stratigraphic trends of PCA scores plotted against lithostratigraphy and calcareous nannofossil biozones. Solid thick curves represent factors extracted from the restricted interval, dotted thin curves represent factors extracted from the entire interval. For lithology legend see Fig. 3.

where their abundance drops to ~40 specimens/mm^2 up to ~14 m, where this taxon disappears.

Genus *Lotharingius* is the only coccolith-genus with abundances comparable to highly calcified nannoliths (*S. punctulata* and *M. jansae*). It shows very low abundances in the Domaro Lmst. and lower portion of the Sogno Fm. (a mean of ~35 specimens/mm^2), although a slight increase is observed across the Pliensbachian/Toarcian boundary. An increase in abundance is observed from 7 m upwards, reaching the highest abundance within the Fish Level (up to 460 specimens/mm^2). In the interval above the black shales *Lotharingius* abundance decreases to values higher than those recorded below the Fish Level (a median of ~100 specimens/mm^2).

The biostratigraphic investigation of smear slides shows that genus *Biscutum* is present from the base of the analysed interval (see Appendix 2). However, the rarity and tiny sizes of *Biscutum* coccoliths prevent their identification in ultrathin sections if abundance is very low. Therefore, *Biscutum* is observed only above 8.3 m, where mean abundances of ~30 specimens/mm^2 are recorded across the Fish Level. In the interval above, abundances are very low (a mean of ~3 specimens/mm^2). Genus *Carinolithus* appears in the earliest Toarcian, and therefore is absent throughout the Domaro Lmst. and the lowermost part of the Sogno Fm. In the first part of its record this genus shows very low abundance (a mean of ~20 specimens/mm^2) and an increase across the Fish Level, reaching values up to ~110 specimens/mm^2. In the portion above the black shale interval *Carinolithus* abundance decreases to values slightly higher than those recorded below the Fish Level (a mean of ~30 specimens/mm^2).

Genus *Calyculus* shows the lowest abundance within the Domaro Lmst. (mean of ~20 specimens/mm^2) and a significant increase from the base of the Sogno Fm. reaching its highest values at 6.0 m (up to 150 specimens/mm^2). *Calyculus* abundance decreases before the Fish Level (a mean of ~50 specimens/mm^2) and displays ample fluctuations across the black shale

A) PCA factors excluding *S. punctulata*				
	FACTOR 1	FACTOR 2	FACTOR 3	interval between the FO of *Carinolithus* and the LO of *M. jansae*
	+ *M. jansae*	+ *Lotharingius*	+ *Calyculus*	
	- *Biscutum/Lotharingius*	- *Crepidolithus*	- *Biscutum*	
AA	78.2% of the variance	20.1% of the variance	1.1% of the variance	
%	60.9% of the variance	35.2% of the variance	2.3% of the variance	
	FACTOR 1	FACTOR 2	FACTOR 3	entire studied interval
	+ *M. jansae*	+ *Lotharingius*	+ *Calyculus*	
	- *Biscutum/Lotharingius*	- *Crepidolithus*	- *Biscutum*	
AA	80.7% of the variance	17.4% of the variance	1% of the variance	
%	68.5% of the variance	27.1% of the variance	2.2% of the variance	

B) PCA factors including *S. punctulata*				
	FACTOR 1	FACTOR 2	FACTOR 3	interval between the FO of *Carinolithus* and the LO of *M. jansae*
	+ *S. punctulata/ M. jansae*	+ *Lotharingius*	+ *M. jansae*	
	- *Biscutum/Lotharingius*	- *Crepidolithus*	- *S. punctulata*	
AA	76.8% of the variance	13% of the variance	9.2% of the variance	
%	54.3% of the variance	32.8% of the variance	10.8% of the variance	
	FACTOR 1	FACTOR 2	FACTOR 3	entire studied interval
	+ *S. punctulata*	+ *S. punctulata*	+ *Lotharingius*	
	- *Biscutum*	- *M. jansae*	- *Crepidolithus*	
AA	80.9% of the variance	11.8% of the variance	6.6% of the variance	
%	64.2% of the variance	23.3% of the variance	11.1% of the variance	

Tab. 2 - PCA factors extracted from calcareous nannofossil absolute abundances (AA) and percentages (%), on both entire and restricted intervals.

interval (0-120 specimens/mm^2). Above the Fish Level, abundance decreases to a mean of ~30 specimens/mm^2.

Genus *Crepidolithus* shows minor fluctuations in abundance with average values of ~45 specimens/mm^2 in the Domaro Lmst. and the lower part of the Sogno Fm. In the Fish Level and the overlying interval *Crepidolithus* abundance decreases to a mean value of ~20 specimens/mm^2.

Principal Component Analyses

The results of PCA applied to both absolute abundances and percentages of the entire studied interval and of the restricted interval (see Materials and Methods for details) are synthetized in Tab. 2 and Fig. 9. The PCA conducted on assemblages without *S. punctulata* extracted three factors, identical for absolute abundances and percentages as well as for the total and restricted stratigraphic intervals. Factor 1 explains the highest variance (60.9-80.7 %) and has the highest positive loading for *M. jansae*, while the lowest negative loading for *Biscutum* and *Lotharingius* (Tab. 2A).

Factor 2 explains 17.4-35.2 % of the variance and displays highest loading for *Lotharingius* opposite to *Crepidolithus*. Factors 1 and 2 together explain ~95-98% of the variance, while Factor 3 corresponds only to 1-2% of the total variance. The latter factor marks the opposition of genus *Calyculus* (highest) to genus *Biscutum* (lowest).

PCA performed on the datasets including *S. punctulata* extracted three factors consistent for absolute abundances and percentages as well as for the total and restricted stratigraphic intervals (Tab. 2B). Factor 1 (54.3-80.9 % of the total variance) displays the highest positive loading for *S. punctulata* and *M. jansae* in opposition to *Biscutum* and *Lotharingius*. We notice that when the total interval is considered, Factor 1 shows highest positive loading for *S. punctulata* opposed to *Biscutum*. Factor 2 of the restricted interval (13-32.8% of the total variance) corresponds to Factor 3 of the total interval (6.6-11.1% of the total variance): they have the highest loading for *Lotharingius* and lowest loading for *Crepidolithus*. Factor 3 of the restricted interval (9.2-10.8% of the total variance) corresponds to Factor 2 of the total interval (11.8-23.3% of the total variance): their loadings are opposite for *S. punctulata* and *M. jansae*.

Paleoecology of Early Jurassic calcareous nannoplankton

The paleoecological affinities of Early Jurassic calcareous nannoplankton are still not well understood

	TAXON	PALEOECOLOGICAL AFFINITY	PCA	AUTHORS
	S. punctulata	oligotrophic	x x (x)	Claps et al. 1995 Cobianchi & Picotti 2001 Pittet & Mattioli 2002 Olivier et al. 2004 Mattioli & Pittet 2004 Erba 2004 Tremolada et al. 2005 Tremolada et al. 2006 Aguado et al. 2008 Reggiani et al. 2010b
		mesotrophic		Mattioli 1997
		deep-dweller		Claps et al. 1995 Erba 2004
		shallow-dweller	(x)	Mattioli 1997 Mattioli & Pittet 2004 Reggiani et al. 2010a
		proximal		Mattioli & Pittet 2004
		warmer temperature	x	Tremolada et al. 2006
		colder temperature	x	Fraguas et al. 2012
Crepidolithus	genus ***Crepidolithus***	oligotrophic	x	Bour et al. 2007
		deep-dweller	x	Bucefalo Palliani et al. 1998 Bour et al. 2007
	***Crepidolithus* spp.** (*C. crassus* and *C. cavus-C. granulatus*)	oligotrophic	x	Fraguas et al. 2012
		deep-dweller	x	Fraguas et al. 2012
	Crepidolithus spp. (*C. cavus, C.* aff. *ocellatus*)	higher latitudes	x	Mattioli et al. 2008
	C. crassus	oligotrophic	x x	Mattioli & Pittet 2004 Aguado et al. 2008 Mattioli et al. 2008
		opportunistic		Walsworth-Bell 2001
		deep-dweller	x x	Tremolada et al. 2005 Mattioli et al. 2008 Reggiani et al. 2010b
		proximal		Mattioli & Pittet 2004
		distal		Reggiani et al. 2010a
		higher latitudes	x	Reggiani et al. 2010b
	M. jansae	oligotrophic		Tremolada et al. 2005
		intermediate-dweller		Erba 2004 Tremolada et al. 2005
		deep-dweller	x x	Bucefalo Palliani et al. 1998 Mattioli & Pittet 2004 Mattioli et al. 2008 Reggiani et al. 2010b Reolid et al. 2014
		lower latitudes	x x	Bucefalo Palliani et al. 2002 Mattioli et al. 2008 Reggiani et al. 2010b
		colder temperature	x x	Fraguas et al. 2012 Clémence et al. 2015
Biscutum	genus ***Biscutum***	mesotrophic	x	Mattioli 1997 Bucefalo Palliani & Mattioli 1995 Mattioli & Pittet 2004 Erba 2004 Bour et al. 2007 Reolid et al. 2014
	***Biscutum* spp.** (*B. finchii, B. novum, B. grande, B. dubium*)	mesotrophic		Tremolada et al. 2005
	***Biscutum* spp.**	mesotrophic	x	Tremolada et al. 2006
	(*B. constans*, B. dubium, B. dorsetensis*)	colder temperature	x	Tremolada et al. 2006
	***Biscutum* spp.** (*B. finchii, B. novum*)	warmer temperature	x	Fraguas et al. 2012
	B. novum	mesotrophic	x	Mailliot et al. 2009 Mattioli et al. 2008
		warmer temperature	x	Clémence et al. 2015
		colder temperature	x	Mattioli et al. 2008
		stress tolerant to anoxia and low salinities	x	Clémence et al. 2015
	B. finchii	mesotrophic	x	Bucefalo Palliani et al. 2002 Mailliot et al. 2009 Mattioli et al. 2008
		colder temperature	x x	Mattioli et al. 2008 Clémence et al. 2015
	B. dubium	mesotrophic	x	Bucefalo Palliani et al. 2002 Aguado et al. 2008
	B. intermedium	mesotrophic	x	Aguado et al. 2008
Lotharingius	genus ***Lotharingius***	mesotrophic		Mattioli & Pittet 2004 Bucefalo Palliani et al. 2002 Reolid et al. 2014
		shallow-dweller		Mattioli & Pittet 2004 Reolid et al. 2014
	***L.otharingius* spp.** (*L. hauffii*, L. crucicentralis, L. velatus, L. sigillatus, L. barozii*)	mesotrophic		Tremolada et al. 2005
	***Lotharingius* spp.** (*L. crucicentralis/sigillatus, L. umbriensis, L. frodoi, L. hauffii*)	mesotrophic	x	Mattioli et al. 2008
		shallow-dweller	x	Mattioli et al. 2008
	***Lotharingius* spp.** (*L. crucicentralis, L.sigillatus, L hauffii*)	shallow-dweller	x	Fraguas et al. 2012
	L. hauffii	mesotrophic	x	Pittet & Mattioli 2002 Olivier et al. 2004 Clémence et al. 2015
	L. sigillatus	mesotrophic	x	Clémence et al. 2015
		warmer temperature	x x	Clémence et al. 2015 Fraguas et al. 2012
	L. crucicentralis	warmer temperature	x	Fraguas et al. 2012
	Calyculus	mesotrophic	x	Mattioli & Pittet 2004 Bour et al. 2007
		shallow-dweller	x	Mattioli et al. 2008 Mattioli et al. 2009
		intermediate-dweller		Erba 2004
		deep-dweller		Bucefalo Palliani & Mattioli 1995
		low salinity	x	Mattioli et al. 2008 Mailliot et al. 2009
		warmer temperature	x	Fraguas et al. 2012
		stress tolerant to anoxia and low salinities	x	Clémence et al. 2015
	Carinolithus	stress tolerant to anoxia and low salinities	x	Clémence et al. 2015

Tab. 3 - Paleoecological affinities of selected Early Jurassic nannoplankton taxa, as reconstructed in previous works. (x): means that the Authors interpreted *Schizosphaerella* but did not include it in the PCA; * highlights the species dominating the genus assemblage, as indicated by the Authors.

and the different interpretations proposed are summarized in Tab. 3 that includes taxa considered in our counts and statistics. On the basis of its size and mass, *S. punctulata* was considered a deep-dweller associated to a deep chlorophyll maximum, like the Cretaceous *Nannoconus* (Erba 2004) in analogy with the extant coccolithophore *Florisphaera profunda* (Molfino & McIntyre 1990), that flourishes in oceanic stable conditions, when the nutricline is deep and, therefore, surface waters are characterized by enhanced oligotrophy. Other Authors interpreted *S. punctulata* a shallow-dweller preferring relatively high nutrients in unstable surface waters, especially in proximal settings. The temperature affinity of this taxon is still controversial, being interpreted as a warmer or colder water form.

Genus *Crepidolithus* was considered a deep-dweller taxon with oligotrophic affinity. In one case *Crepidolithus* spp. *(C. cavus* and *C.* aff. *C. ocellatus*) was interpreted as preferring higher latitudes. Different paleoecological interpretations were proposed for *C. crassus*: most Authors indicate this taxon as oligotrophic and deep-dweller. Some Authors reconstructed preferences for distal or proximal settings, perhaps with affinity for higher latitudes. A single paper considers *C. crassus* as an opportunistic taxon proliferating under unstable fertile conditions.

Most Authors (Tab. 3) interpreted *M. jansae* as a deep to intermediate-dweller. Other paleocological recontructions proposed affinity for oligotrophic areas, lower latitudes or colder temperatures.

The Early Jurassic genus *Biscutum* was interpreted similarly to the Cretaceous species *Biscutum constans* (Roth & Krumbach 1986; Erba 1992; Herrle et al. 2003; Mutterlose et al. 2005), considered a higher fertility indicator. The suggested paleotemperature affinities are questionable, because opposed interpretations were forwarded. As fas as single species are concerned, a common preference for mesotrophic conditions was derived, for *B. novum*, *B. finchii*, *B. dubium* and *B. intermedium*. In addition some control by surface water temperature was pointed out for *B. novum*, although affinity for both warmer and colder conditions were proposed. Some preference for colder water was suggested for *B. finchii.* Recently, *B. novum* was interpreted as stress tolerant to anoxia and low salinities.

The genus *Lotharingius* was interpreted as a shallow-dweller and higher fertility taxon, usually asso-

ciated to *Biscutum*. Both *L. hauffii* and *L. sigillatus* were found to be favored by mesotrophic conditions, while *L. sigillatus* and *L. crucicentralis* were associated to warmer temperature.

Genus *Calyculus* was considered a shallow, intermediate or deep-dweller, with preference for higher nutrient concentrations, and possibly adapted to lower salinity. Only in one case the genus *Calyculus* was associated to warmer temperature. In a recent study by Clémence et al. (2015) genera *Calyculus* and *Carinolithus* were considered tolerant to anoxia and low salinities.

As a general remark, the screening of previous literature on the paleoecology of Early Jurassic calcareous nannoplankton suggests that in most cases the significance of single species largely corresponds to the affinity interpreted for the genus.

Previous works using PCA for Jurassic nannofossil assemblages (Tremolada et al. 2006; Bour et al. 2007; Aguado et al. 2008; Mattioli et al. 2008; Reggiani et al. 2010b; Fraguas et al. 2012; Clémence et al. 2015) extracted factors very similar to those obtained in this study, and interpreted as related to fertility (nutricline depth and intensity), position of nannoplankton groups in the photic zone, or salinity of surface water masses.

When *S. punctulata* is excluded from the assemblages, our Factors 1 and 2 seem both associated to fertility, although with some degree of differentiation. Specifically, Factor 1 extracts the mesotrophic shallow-dwellers *Biscutum* and *Lotharingius* opposite to the intermediate-dweller *M. jansae.* As discussed above, the paleoecological affinities of individual species within *Lotharingius* and *Biscutum* are mostly consistent with the reconstructed preference of the genera. Therefore, our interpretations are largely in agreement with previous works (Mattioli et al. 2008; Fraguas et al. 2012; Clémence et al. 2015). We interprete our Factor 2 opposing *Lotharingius* to *Crepidolithus* as related to a more specific control by nutrients on surface (*Lotharingius*) versus intermediate (*Crepidolithus*) dwellers, similarly to previous reconstructions (Aguado et al. 2008; Mattioli et al. 2008). However, we notice that in previous PCA analyses (Mattioli et al. 2008; Clémence et al. 2015) *L. hauffii* was also extracted together with *C. crassus* and interpreted as related to a stratified ocean with the nutricline at intermediate depth within the photic zone.

In the Colle di Sogno section, we also detected a Factor 3 opposing *Calyculus* and *Biscutum* as previously found by Bour et al. (2007), who provided an interpretation of nutricline position. However, following the reconstructions of Mattioli et al. (2008) and Clémence et al. (2015) suggesting that *Calyculus* might be favoured by lower salinity we interpret our Factor 3 as indicative of changing run-off and therefore salinity of surface waters.

The factors obtained from the dataset including *S. punctulata*, partly overlap those extracted excluding *S. punctulata*. In fact, Factor 1 opposing *S. punctulata* and *M. jansae* to *Biscutum* and *Lotharingius* is interpreted as deriving from nutricline position and intensity, with *M. jansae* and *S. punctulata* taking advantage of a deep nutricline in the intermediate to lower part of the photic zone, respectively. Other Authors found *Schizosphaerella* opposed to *Biscutum*: Aguado et al. (2008) interpreted this opposition reflecting nutricline depth, whereas Tremolada et al. (2006) highlighted a possible influence of colder temperature or higher salinity on *Biscutum.*

Our factor 2 is identical for the datasets excluding and including *S. punctulata* (Fig. 9, Tab. 2). We speculate that Factor 3, opposing *M. jansae* and *S. punctulata* records the competition between these two taxa in the middle to lower part of the photic zone. Specifically, *S. punctulata* occupied a deeper position profiting of a deeper nutricline, while *M. jansae* was an intermediate-dweller flourishing with a relatively shallower nutricline.

Figure 9 illustrates the factors and their scores obtained for the total investigated interval as well as for the interval comprised between the FO of *Carinolithus* and the LO of *M. jansae*, pointing out identical results. The factor scores highlight trends and changes primarily associated to the Fish Level interval that is distinguished from the underlying and overlying portions of the section. After conditions of relative stability and oligotrophy (Factors 1 and 2), a rapid shift to higher nutrient content (Factors 1 and 2) and perhaps lower salinity (Factor 3 excluding *S. punctulata*) marks the deposition of dysoxic to anoxic sediments. Above the Fish Level, a return to a deeper nutricline (Factors 1 and 2) remains apparently associated to lower salinity (Factor 3 excluding *S. punctulata*) of surface waters.

Paleoceanographic reconstruction of the Late Pliensbachian-Early Toarcian time interval at local, regional and global scale

Our results confirm and partly implement the paleoecological affinities of some Early Jurassic nannoplankton taxa. As expected, a large influence was exerted by fertility of surface waters and in Fig. 10 we synthetize the possible distribution of *Lotharingius*, *Biscutum*, *Calyculus*, *Carinolithus*, *Crepidolithus*, *M. jansae* and *S. punctulata* relative to their depth within the photic zone in areas of stability (thermocline and deep nutricline) and instability (surface nutricline). Concurrent paleoecological factors were presumably

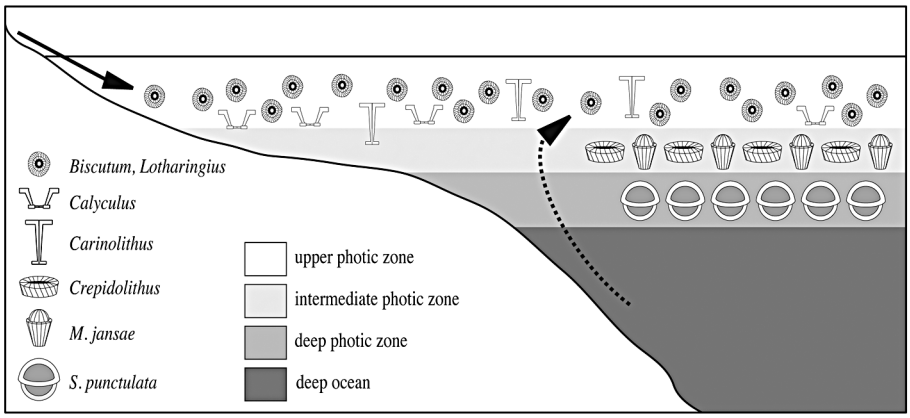

Fig. 10 - Inferred position of some Early Toarcian nannoplankton taxa within the photic zone. Arrows indicate nutrient fluxes via run-off (solid line) and upwelling (dotted line).

temperature and salinity, but limited support is available for Early Jurassic times. *M. jansae* might have preferred colder waters, while *Calyculus*, *B. finchii*, *L. crucicentralis* and *L. sigillatus* seem more adapted to warmer temperature (Tab. 3). Another factor controlling abundance and type of nannoplankton is CO_2 concentration in the atmosphere-ocean system that influences calcification rates. Heavily calcified *S. punctulata* and *M. jansae* were conceivably disadvantaged under higher CO_2 (and relative ocean acidification), while taxa producing smaller and less calcified coccoliths were favoured (e.g. Erba 2004, 2006; Mattioli et al. 2004; Tremolada et al. 2005; Suan et al. 2008; Fraguas & Young 2011).

The paleoceanographic conditions in the Late Pliensbachian-Early Toarcian time interval at Colle di Sogno are here reconstructed using changes in nannofossil absolute abundances and scores of PCA factors (Figs 8-9). In the Lombardy Basin, during the latest Pliensbachian stable oligotrophic conditions promoted the proliferation of deep-dwelling and highly calcified *S. punctulata* and *M. jansae*. At the beginning of the Toarcian enhanced continental run-off is evidenced by a significant increase of terrigenous input with, presumably, twofold effects. A decreased light penetration penalized the deep-dweller *S. punctulata*, favouring the intermediate-dweller *M. jansae*. At the same time, accelerated run-off induced lower salinity and an increase of *Calyculus*.

In the studied area, the onset of the T-OAE corresponds to higher concentration of nutrients, apparently associated with lower salinity and perhaps warmer waters stimulating the proliferation of shallow, mesotrophic coccolith-producers (particularly *Biscutum* and *Lotharingius*) and favoring *Calyculus*, but hampering deep- to intermediate-dwelling, oligotrophic forms (*S. punctulata*, *M. jansae* and *Crepidolithus*). The slight increase in abundance of *Carinolithus* within the Fish Level (Fig. 8) suggests two hypotheses: this taxon preferred higher nutrient concentrations, or was adapted to lower salinity.

We notice that paleoenvironmental changes shortly preceded the onset of the major perturbation, as evidenced by a relative increase in *Lotharingius* abundance and Factor 2 scores below the $\delta^{13}C$ anomaly (Figs 8-9). However, some condensation is observed in the interval preceding the Fish Level and nannofossil abundances might derive from differential dissolution.

After the deposition of black shales in the Lombardy Basin, calcareous nannoplankton only partly recovered in abundance and diversity, possibly suggesting residual perturbed conditions. In fact, scores of PCA Factors 2 and 3 remain relatively high for the fertility-related *Lotharingius* and *Biscutum* and for the lower-salinity *Calyculus*, suggesting that stable conditions and a deep nutricline were not restored.

Our data are mostly consistent with nannofossil abundance, diversity and dominance documented in central Tethys (Claps et al. 1995; Erba 2004; Mattioli et al. 2004, 2008, 2009), in the westernmost Tethys (Mattioli et al. 2008, 2009; Suan et al. 2008, 2010; Reolid et al. 2014), in Portugal and N Spain (Tremolada et al. 2005; Mattioli et al. 2008, 2009; Fraguas & Young 2011; Fraguas et al. 2012), and partly in the Boral/subBoreal region (Bucefalo Palliani et al. 2002; Mattioli et al.. 2004, 2008, 2009; Hermoso et al. 2009a; Mailliot et al. 2009; Clémence et al. 2015). Although some specific patterns characterize individual sections as a result of local paleoceanographic changes, at supraregional scale the latest Pliensbachian was characterized by the dominance of *S. punctulata* and *M. jansae* suggesting stable, oligotrophic, relatively cool conditions (Claps et al. 1995; Tremolada et al. 2005; Suan et al. 2010; Fraguas et al. 2012; Reolid et al. 2014). At the beginning of the Toarcian a decrease in abundance of *S. punctulata* and locally of *M. jansae* is registered together with an increase of *Biscutum* and *Lotharingius* (Tremolada et al. 2005; Mattioli et al. 2008, 2009; Fraguas et al. 2012; Reolid et al. 2014). There is a general consensus for an initial relative increase in nutrient availability, possibly introduced by higher run-off, and warming.

The "*Schizosphaerella* decline" at the Pliensbachian/Toarcian boundary recorded at supraregional scale (Erba 2004; Tremolada et al. 2005; Mattioli et al. 2008; Suan et al. 2008) suggests a global cause. Although higher fertility might have induced a reduction of oligotrophic forms, calcification failure under increased atmospheric pCO_2 and some ocean acidification were proposed as main triggering mechanism (Erba 2004, 2006; Tremolada et al. 2005; Mattioli et al. 2008; Suan et al. 2008). In this study, at the Pliensbachian/Toarcian boundary we also notice a decrease of the "encrusted *S. punctulata*" that, as it is the most calcified form, might have been the morphotype most sensitive to acidification. At the same level a decrease in size of *S. punctulata* is reported from various basins (Mattioli et al. 2004, 2009; Suan et al. 2008, 2010).

The nannoplankton patterns indicate a significant paleoenvironmental change just before the onset of the T-OAE recorded by the most dramatic shift in assemblage composition reaching a climax during the anoxic interval. The extreme paleoenvironmental conditions produced by fertilization, fresh water input, warming and relative acidification contributed to the establishment and maintenance of very stressing surface waters with overwhelming opportunistic taxa. Ocean acidification might have reached threshold values at the onset of the T-OAE inducing the "*Schizosphaerella* crisis", the exclusion of "encrusted *S. punctulata*" and the survival of exclusively "thin *M. jansae*" (Figs 8-9). The size reduction in *Schizosphaerella* (Mattioli et al. 2004, 2009; Suan et al. 2008, 2010; Clémence et al. 2015) and *Lotharingius* (Fraguas & Young 2011) were arguably also related to unfavourable condition for biomineralization under ocean acidification.

Although our dataset does not allow reconstructions of paleotemperature trends, previous works documented a significant warming across the T-OAE (e.g. Jenkyns 2010) presumably induced by the emplacement of the Karoo-Ferrar province at ~183 Ma (e.g. Ikeda & Hori 2014), that might have introduced excess CO_2 causing a climate change as speculated by previous Authors (Erba 2004; Mattioli et al. 2004, 2009; Tremolada et al. 2005; Suan et al. 2008; Fraguas et al. 2012; Hermoso et al. 2009b; Clémence et al. 2015). Data from the Colle di Sogno section confirm that the T-OAE was a weathering-induced nutrification episode combined with ocean acidification due to excess CO_2 exerting a direct control on phytoplankton type and abundance.

Environmental stress started to affect the ocean structure, fertility and chemistry at least 1 million years before the T-OAE, close to the Pliensbachian/Toarcian boundary, and was marked by precursor steps of perturbation culminating into a biological-chemical-physical crisis (Wignall et al. 2005; Suan et al. 2010). The nannoplankton speciation episode, the most important one for calcareous nannoplankton within the Mesozoic (Bown et al. 2004; Erba 2006), is testified by accelerated rates in nannoplankton origination (mainly placoliths) in the latest Pliensbachian-Early Toarcian interval. Although dramatic transient changes in nannofloral communities are recorded worldwide, the environmental perturbations preceding and accompanying the T-OAE had also some positive effects on calcareous nannoplankton evolution by stimulating calcification of new coccolith morphologies.

After the T-OAE, paleoceanographic conditions only partly and gradually returned to the pre-perturbation state, at least as far as the photic zone is concerned. All available data testify nannoplankton assemblages with relatively abundant *Crepidolithus*, *Biscutum* and *Lotharingius* and a minor recovery of *Schizophaerella* and total nannofloral abundance suggesting that the deepening of the nutricline and stratification of calcareous phytoplankton through the photic zone required a long period after anoxia terminated (Tremolada et al. 2005; Mattioli et al. 2008, 2009; Fraguas et al. 2012; Mailliot et al. 2009; Clémence et al. 2015; Reolid et al. 2014; this study).

Conclusions

The calcareous nannofossil biostratigraphy of the Colle di Sogno section allowed the identification of seventeen biohorizons spanning the latest Pliensbachian-Early Toarcian interval. The zonation proposed for the Tethyan realm (Mattioli & Erba 1999) was successfully applied and NJT 5 and NJT 6 zones were identified. The sequence of nannofossil biohorizons is mostly consistent with data available from different areas at lower and higher latitudes, although only few of them can be used for inter-regional correlations. The apparent discrepancies obtained through calibration of the nannofossil events against ammonite zones are in part overcome by the correlation to the C isotopic chemostratigraphy of the Early Toarcian. Few nannofossil events constrain the T-OAE C isotopic anomaly and are traceable among different regions. The appearance of *C. superbus* correlates with the onset of the T-OAE, while the FO of *D. striatus* postdates the end of the C isotopic anomaly. The dataset regarding the disappearance level of *M. jansae* allowed the separation of its LCO preceding the LO. The LCO of *M. jansae* is more evident at lower latitudes where a major abundance decrease marks the onset of T-OAE C isotopic anomaly. At similar stratigraphic levels, the LO of *M. jansae* is reported at higher latitudes. We propose here the LO of *M. jansae* as additional event to approximate the end of the T-OAE at lower latitudes. Quantitative investigation of ultrathin sections revealed major changes in ab-

solute abundances of total nannofloras and individual taxa; in particular, the "*Schizosphaerella* decline" and "*Schizosphaerella* crisis" are here suggested as additional biohorizons to approximate the Pliensbachian/Toarcian boundary and the T-OAE onset, respectively.

The PCA, performed on assemblages including and excluding *S. punctulata*, extracted three factors attributed to surface water stability/instability, fertility and salinity. Our results confirm and partly implement previous reconstructions of nannoplankton paleoecology that are used to trace the environmental evolution across the T-OAE at local, regional and global scales.

During the latest Pliensbachian stable oligotrophic conditions promoted the proliferation of deep-dwelling and highly calcified *S. punctulata* and *M. jansae* in the Lombardy Basin and in general at lower latitudes. Ecosystem perturbations started in the earliest Toarcian with generally enhanced nutrient availability and possibly lower salinity, evidenced by a significant increase in terrigenous input in the Lombardy Basin. The "*Schizosphaerella* decline" at the Pliensbachian/Toarcian boundary recorded at supraregional scale is inferred to be related also to partial calcification failure under CO_2-induced ocean acidification. At global scale, paleoenvironmental stress due to a combination of nutrification, disruption of surface water stability, lower salinity and excess CO_2 reached threshold values inducing a rapid turnover of assemblages just before the beginning of the T-OAE. During this event, prolonged meso- to eutrophic conditions associated to lower salinity and possibly warmer waters favoured *Lotharingius*, *Biscutum* and *Calyculus* while ocean acidification arguably hampered calcification of *S. punctulata* and *M. jansae* at local to supraregional scales. Available data indicate that after the T-OAE, the recovery of k-selected deep- and intermediate-dwellers required a long period after anoxia terminated.

Data from the Colle di Sogno section confirm that the T-OAE was a nutrification episode combined with some ocean acidification exerting a direct control on phytoplankton type and abundance. A general consensus indicates the emplacement of the Karoo-Ferrar province as crucial for the Early Toarcian paleoclimatic and paleoceanographic changes. Stressing conditions started in the latest Pliensbachian and triggered subsequent changes in nannofloral composition and structure recorded worldwide, associated to accelerated rates in nannoplankton origination suggesting that the environmental perturbations preceding and accompanying the T-OAE possibly stimulated biomineralization of new coccolith morphologies.

Acknowledgements. This paper is one of the results of C.E.C.'s Post-Doc, co-funded by Università degli Studi di Milano and European Social Found (FSE), and supported by PRIN prot. 2010X3PP8J_001 to E.E. G. Faucher is acknowledged for help in the field. This paper benefited of the valuable reviews and thoughtful comments of Silvia Gardin and Angela Fraguas.

REFERENCES

Aguado R., O'Dogherty L. & Sandoval J. (2008) - Fertility changes in surface waters during the Aalenian (mid-Jurassic) of the Western Tethys as revealed by calcareous nannofossils and carbon-cycle perturbations. *Mar. Micropaleontol.,* 68: 268-285.

Al-Suwaidi A.H., Angelozzi G.N., Baudin F., Damborenea S.E., Hesselbo S.P., Jenkyns H.C., Manceñido M.O. & Riccardi A.C. (2010) - First record of the Early Toarcian Oceanic Anoxic Event from the Southern Hemisphere, Neuquén Basin, Argentina. *J. Geol. Soc. London*, 167: 633-636.

Baccelle L. & Bosellini A. (1965) - Diagrammi per la stima visiva della composizione percentuale nelle rocce sedimentarie. *Ann. Univ. Ferrara*, Sezione IX 1/3, 59-62.

Baldanza A. & Mattioli E. (1992) - Biostratigraphical synthesis of nannofossils in the Early Middle Jurassic of Southern Tethys. *Knihovnicka, ZPN*, 14a, 1: 111-141.

Baldanza A., Bucefalo Palliani R. & Mattioli E. (1995) - Lower Jurassic calcareous nannofossils and dynoflagellate cysts of Hungary and their comparison with assemblages from Central Italy. *Palaeopelagos,* 5: 161-174.

Bassoullet J.P., Elmi S., Poisson A., Cecca F., Bellion Y., Guiraud R. & Baudin F. (1993) - Mid Toarcian. In: Dercourt J., Ricou L.E. & Vrielynck B. (Eds) - Atlas Tethys Paleoenvironmental Maps. *BEICIP- FRANLAB*: 63-84, Rueil-Malmaison, France.

Baumgartner P.O., Bernoulli D. & Martire L. (2001) - Mesozoic pelagic facies of the Southern Alps: Paleotectonics and paleoceanography. *IAS 2001 Davos, Fieldtrip Guide*, Excursion A1, Davos.

Beaufort L. & Heussner S. (2001) - Seasonal dynamics of calcareous nannoplankon on a west European continental margin: The Bay of Biscay. *Mar. Micropaleontol.*, 43: 27-55.

Bodin S., Mattioli E., Fröhlich S., Marshall J.D., Boutib L., Lahsini S. & Redfern J. (2010) - Toarcian carbon isotope shifts and nutrient changes from the Northern margin of Gondwana (High Atlas, Morocco, Jurassic): Paleoenvironmental implications. *Palaeogeogr., Palaeoclimatol., Palaeoecol.*, 297: 377-390.

Boulila S., Galbrun B., Huret E., Hinnov L.A., Rouget I., Gardin S. & Bartolini A. (2014) - Astronomical calibration of the Toarcian Stage: Implications for sequence stratigraphy and duration of the early Toarcian OAE. *Earth Planet. Sci. Lett.,* 386: 98-111.

Bour I., Mattioli E. & Pittet B. (2007) - Nannofacies analysis as a tool to reconstruct paleoenvironmental changes during the Early Toarcian anoxic event. *Paleogeogr. Paleoclimatol. Palaeoecol.*, 249: 58-79.

Bown P.R. (1987) - Taxonomy, evolution and biostratigraphy of Late Triassic-Early Jurassic calcareous nannofossils. *Palaeont. Ass., Special pap. Paleontol.,* 32, 118 pp.

Bown P.R. (1992) - Late Triassic-Early Jurassic calcareous nannofossils of the Queen Charlotte Islands, British Columbia. *J. Micropalaeontol.,* 11(2): 177-188.

Bown P.R. & Cooper M.K.E. (1989) - Conical calcareous nannofossils in the Mesozoic. In: Crux J.A. & Van Heck S.E. (Eds) - Nannofossils and their applications. *Proc. Intern. Nannofossil Ass. Conf., London 1987*: 98-106, London.

Bown P.R. & Cooper M.K.E. (1998) - Jurassic. In: Bown P.R. (Ed.) - Calcareous nannofossil biostratigraphy. *British Micropaleontol. Soc. Pub. Series*: 34-85. Kluwer Academic Publishers, London.

Bown P.R., Cooper M.K.E. & Lord A.R. (1988) - A calcareous nannofossil biozonation scheme for the early to mid Mesozoic. *Newsl. Stratigr.,* 20: 91-114.

Bown P.R., Lees J.A. & Young J.R. (2004) - Calcareous nannoplankton evolution and diversity through time. In: Thierstein H.R. & Young J.R. (Eds) - Coccolithophores: from molecular processes to global impact: 481-508, Berlin.

Bucefalo Palliani R. & Mattioli E. (1995) - Ecology of dinoflagellate cysts and calcareous nannofossils from bituminous facies of the Early Toarcian, central Italy. *Europal Newsl.,* 8: 60-62.

Bucefalo Palliani R. & Mattioli E. (1998) - High resolution integrated microbiostratigraphy of the Lower Jurassic (late Pliensbachian-earlyToarcian) of central Italy. *J. Micropaleontol.*, 17: 153-172.

Bucefalo Palliani R., Cirilli S. & Mattioli E. (1998) - Phytoplankton response and geochemical evidence of the lower Toarcian relative sea-level rise in the Umbria-Marche basin (Central Italy). *Palaeogeogr., Palaeoclimatol., Palaeoecol.,* 142: 33-50.

Bucefalo Palliani R., Mattioli E. & Riding J.B. (2002) - The response of marine phytoplankton and sedimentary organic matter to the Early Toarcian (Lower Jurassic) oceanic anoxic event in northern England. *Mar. Micropaleontol.,* 46: 223-245.

Burnett J.A. (1998) - Upper Cretaceous. In: Bown P.R. (Eds) - Calcareous Nannofossil Biostratigraphy. *British Micropaleontol. Soc. Pub. Series. Kluwer Acad. Pub.*: 132-199.

Channell J.E.T., Casellato C.E., Muttoni G. & Erba E. (2010) - Polarity and polar wander at the Jurassic-Cretaceous boundary in the Southern Alps, Italy. *Paleogeogr., Paleoclimatol., Palaeoecol.*, 293: 51-75.

Claps M., Erba E., Masetti D. & Melchiorri F. (1995) - Milankovitch-type cycles recorded in Toarcian black shales from Belluno Trough (Southern Alps, Italy). *Mem. Soc. Geol.,* 47: 179-188.

Clémence M.E., Gardin S., Bartolini A. (2015) - New insights in the pattern and timing of the Early Jurassic calcareous nannofossil crisis. *Paleogeogr., Paleoclimatol., Palaeoecol.*, 427: 100-108.

Cobianchi M. (1990) - I Nannofossili calcarei del Sudalpino occidentale: biostratigrafia, cronostratigrafia e influenza di eventi di ordine abiotico. PhD thesis, University of Pavia.

Cobianchi M. (1992) - Sinemurian-Early Bajocian calcareous nannofossil biostratigraphy of the Lombardian Basin (Southern calcareous Alps; Northern Italy). *Att. Ticin. Sci. Terra,* 35: 61-106.

Cobianchi M. & Picotti V. (2001) - Sedimentary and biological response to sea-level and paleocenographic changes of a Lower-Middle Jurassic Tethyan platform margin (Southern Alps, Italy). *Paleogeogr., Paleoclimatol., Palaeoecol.*, 169: 219-244.

Cobianchi M., Erba E. & Pirini Radrzzani C. (1992) - Evolutionary trends of calcareous nannofossil genera *Lotharingius* and *Watznaueria* during the Early and Middle Jurassic. *Mem. Sci. Geol.,* 43: 19-25.

Covington J.M. & Wise S.W. (1987) - Calcareous Nannofossil biostratigraphy of a Lower Cretaceous Deep-Sea fan complex: Deep Sea Drilling Project Leg 93 Site 603, lower continental rise off Cape Hatteras. *Init. Rep. DSDP*, 93: 617-660.

de Kaenel E. & Bergen J.A. (1993) - New Early and Middle Jurassuc coccolith taxa and biostratigraphy from the eastern proto-Atlantic (Morocco, Portugal and DSDP Site 547 B). *Eclogae Geol. Helv.,* 86: 861-907.

de Kaenel E., Bergen J.A. & Perch-Nielsen K. (1996) - Jurassic calcareous nannofossil biostratigraphy of Western Europe. Compilation of recent studies and calibration of bioevents. *Bull. Soc. Géol. Fr.,* 167(1): 15-28.

Deflandre G. & Dangeard L. (1938) - *Schizosphaerella,* un nouveau microfossile méconnudu Jurassique moven et supérieur. *C.R. Acad. Sci. Paris,* 207: 115-1117.

Dunham R.J. (1962) - Classification of carbonate rocks according to depositional texture. *AAPG Mem.*, 1:108-121.

Elmi S., Gabilly J., Mouterde R., Rulleau L. & Rocha R.B. (1993) - L'étage Toarcien de l'Europe et de la Téthys: divisions et correlations. *Geobios*, 17: 149-159.

Erba E. (1992) - Middle Cretaceous calcareous nannofossils from the western Pacific (Leg 129): evidence for paleoequatorial crossings. *Proc. ODP, Sci. Result,* 129: 189-201.

Erba E. (1994) - Nannofossils and superplumes: the Early Aptian "nannoconid crisis". *Paleoceanography,* 9(3): 483-501.

Erba E. (2004) - Calcareous nannofossils and Mesozoic oceanic anoxic events. *Mar. Micropaleontol.,* 52: 85-106.

Erba E. (2006) - The first 150 million years history of calcareous nannoplankton: Biosphere - Geosphere interac-

tion. *Paleogeogr., Paleoclimatol., Palaeoecol.*, 232: 237-250.

Erba E. & Cobianchi M.A. (1989) - Upper Carixian to Lower Bajocian nannobiohorizons identified in the Lombardy Basin. In: Clari P.A., Cobianchi M.A., Erba E., Gaetani M., Martire L. & Pavia G. (Eds) - Escursione sul Giurassico delle Alpi Meridionali, 24-28 settembre, Milano

Erba E. & Tremolada F. (2004) - Nannofossil carbonate fluxes during Early Cretaceous: phytoplankton response to nutrification episodes, atmospheric CO_2, and anoxia. *Paleoceanography,* 19, PA1008, doi:10.1029/2003PA000884.

Fraguas A. & Young J.R. (2011) - Evolution of the coccolith genus *Lotharingius* during the Late Pliensbachian-Early Toarcian interval in Asturias (N Spain). Consequences of the Early Toarcian environmental perturbations. *Geobios*, 44: 361-375.

Fraguas A., Comas-Rengifo M.J. & Perilli N. (2008) - Pliensbachian calcareous nannofossils of the Santotis section (Basque-Cantabrian Basin, N Spain). *Atti Soc. tosc. Sci. nat., Mem., Serie A,* 113: 49-56.

Fraguas A., Comas-Rengifo M.J., Gómez J. & Goy A. (2012) - The calcareous nannofossil crisis in Northern Spain (Asturias province) linked to the Early Toarcian warming-driven mass extinction. *Mar. Micropaleontol.,* 94-95: 58-71.

Fraguas A., Comas-Rengifo M.J. & Perilli N. (2015) - Calcareous nannofossil biostratigraphy of the Lower Jurassic in the Cantabrian Range (Northern Spain). *Newsl. Stratigr.*, 48(2): 179-199.

Fukunaga K. (1990) - Introduction to Statistical Pattern Recognition. Elsevier, Amsterdam, 592 pp.

Gaetani M. & Poliani G. (1978) - Il Toarciano e il Giurassico medio in Albenza (Bergamo). *Riv. It. Paleontol. Strat.*, 84(2): 349-382.

Gardin S. & Manivit H. (1994) - Biostratigraphie des nannofossiles clacaires du Toarcien du Quercy (Sud-Ouest de la France). Comparison avec la coupe stratotypique de la cimenterie d'Airvault (Deux-Sèvres, France). *Geobios*, M.S. 17: 229-244.

Hammer Ø., Harper D.A.T. & Ryan P.D. (2001) - PAST: Paleontological Statistics Software Package for Education and Data Analysis. *Palaeontol. Elect.* 4(1): 9.

Hermoso M., Le Callonnec L., Minoletti F., Renard M. & Hesselbo S.P. (2009a) - Expression of the Early Toarcian negative carbon-isotope excursion in separated carbonate microfractions (Jurassic, Paris Basin). *Earth Planet. Sci. Lett.,* 277: 194-203.

Hermoso M., Minoletti F., Le Callonnec L., Jenkyns H.C., Hesselbo S.P., Rickaby R.E.M., Renard M., de Rafélis M. & Emmanuel L. (2009b) - Global and local forcing of Early Toarcian seawater chemistry: A comparative study of different paeoceanographic settins (Paris and Lusitanian Basins). *Paleoceanography*, 24, PA4208, doi:10.1029/2009PA001764.

Hermoso M., Minoletti F., Rickaby R.E.M., Hesselbo S.P., Baudin F. & Jenkyns H.C. (2012) - Dynamics of a stepped carbon-isotope excursion: Ultra high-resolution study of Early Toarcian environmental change. *Earth Planet. Sci. Lett.*, 319-320: 45-54.

Herrle J.O., Pross J., Friedrich O., Kößler P. & Hemleben C. (2003) - Forcing mechanisms for mid-Cretaceous black shale formation: evidence from the Upper Aptian and Lower Albian of the Vocontian Basin (SE France). *Paleogeogr., Paleoclimatol., Palaeoecol.*, 190: 399-426.

Hesselbo S.H., Gröcke D.R., Jenkyns H.C., Bjerrun C.J., Farrimond P., Morgans Bell H.S. & Green O.R. (2000) - Massive dissociation of gas hydrate during a Jurassic oceanic anoxic event. *Nature,* 406: 392-395.

Hesselbo S.H., Jenkyns H.C., Duarte L.V. & Oliveira L.C.V. (2007) - Carbon-isotope record of the Early Jurassic (Toarcian) Oceanic Anoxic Event from fossil wood and marine carbonate (Lusitanian Basin, Portugal). *Earth Planet. Sci. Lett.*, 253: 455-470.

Ikeda M. & Hori R.S. (2014) - Effects of Karoo-Ferrar volcanism and astronomical cycles on the Toarcian Oceanic Anoxic Events (Early Jurassic). *Paleogeogr., Paleoclimatol., Palaeoecol.*, 410: 134-142.

Jenkyns H.C. (1988) - The Early Toarcian (Jurassic) anoxic event: stratigraphic, sedimentary, and geochemical evidence. *Am. J. Sci.,* 288: 101-151.

Jenkyns H.C. (2003) - Evidence for rapid climate change in the Mesozoic-Palaeogene greenhouse world. *Phil. Trans. R. Soc. Lond. A*, 361: 1885-1916.

Jenkyns H.C. (2010) - Geochemistry of ocean anoxic events. *Geochem., Geophys., Geosyst.,* 11(3), doi:10.1029/2009GC002788.

Jenkins H.C. & Clayton C.J. (1986) - Black shales and carbon isotopes in pelagic sediments from the Tethyan Lower Jurassic. *Sedimentology,* 33: 87-106.

Jenkyns H.C., Sarti M., Masetti D. & Howarth M.K. (1985) - Ammonites and stratigraphy of Lower Jurassic black shales and pelagic limestones from the Belluno Trough, Southern Alps, Italy. *Eclogae geol. Helv.,* 78(2): 299-311.

Jenkyns H.C., Jones C.E., Gröcke D.R., Hesselbo S.P. & Parknson D.N. (2002) - Chemostratigraphy of the Jurassic System: applications, limitations and implications for palaeoceanography. *J. Geol. Soc. London,* 159: 351-378.

Kafousia N., Karakitsios V., Mattioli E., Kenjo S. & Jenkyns H.C. (2014) - The Toarcian Oceanic Anoxic Event in the Ionian Zone, Greece. *Palaeogeogr., Palaeoclimatol., Palaeoecol.,* 393: 135-145.

Kälin O. (1980) - *Schizosphaerella punctulata* Deflandre & Dangeard: wall ultrastructure and preservation in deep-water carbonate sediments of the Tethyan Jurassic. *Eclogae Geol. Helv.,* 73(3): 983-1008.

Kälin O. & Bernoulli D. (1984) - *Schizosphaerella* Deflandre & Dangeard in Jurassic deeper-water carbonate sediments, Mazagan Continental margin (Hole 547B) and Mesozoic Tethys. *Init. Rep. DSDP,* 79: 411-429.

Lozar F. (1995) - Calcareous nannofossil biostratigraphy of Lower Liassic from Western Tethys. *Paleontographia Italica,* 82: 91-121.

Mailliot S., Mattioli E., Guex J. & Pittet B. (2006) - The Early Toarcian anoxia, a synchronous event in the

Western Tethys? An approach by quantitative biochronology (Unitary Associations), applied on calcareous nannofossils. *Palaeogeogr., Palaeoclimatol., Palaeoecol.*, 240: 562-586.

Mailliot S., Mattioli E., Bartolini A., Baudin F., Pittet B. & Guex J. (2009) - Late Pliensbachian-Early Toarcian (Early Jurassic) environmental changes in an epicontinental basin of NW Europe (Causses area, central France): A micropaleontological and geochemical approach. *Palaeogeogr., Palaeoclimatol., Palaeoecol.*, 273: 346-364.

Mattioli E. (1996). New calcareous nannofossil species from the Early Jurassic of Tethys. *Riv. It. Paleontol. Strat.,* 102(3): 397-412.

Mattioli E. (1997) - Nannoplankton productivity and diagenesis in the rithmically bedded Toarcian-Aalenian Fiuminata section (Umbria-Marche Apennine, Central Italy). *Palaeogeogr., Palaeoclimatol., Palaeoecol.*, 130: 113-133.

Mattioli E. & Erba E. (1999) - Synthesis of Calcareous Nannofossil events in Tethyan Lower and Middle Jurassic successions. *Riv. It. Paleontol. Strat.,* 105(3): 343-376.

Mattioli E. & Pittet B. (2002) - Contribution of calcareous nannoplankton to carbonate deposition: a new approach applied to the Lower Jurassic of Central Italy. *Mar. Micropaleontol.,* 45: 175-190.

Mattioli E. & Pittet B. (2004) - Spatial and temporal distribution of calcareous nannofossils along a proximal-distal transect in the Lower Jurassic of the Umbria-Marche Basin (Central Italy). *Palaeogeogr., Palaeoclimatol., Palaeoecol.*, 205: 295-316.

Mattioli E., Pittet B., Bucefalo Palliani R., Röhl H.J., Schmid-Röhl A. & Morettini E. (2004) - Phytoplankton evidence for the timing and correlation of paleoceanographical changes during the early Toarcian oceanic anoxic event (Early Jurassic). *J. Geol. Soc. London,* 161: 685-693.

Mattioli E., Pittet B., Suan G. & Mailliot S. (2008) - Calcareous nannoplankton changes across the early Toarcian oceanic anoxic event in the western Tethys. *Paleoceanography,* 23, PA3208, doi:10.1029/2007PA001435.

Mattioli E., Pittet B., Petitpierre L. & Mailliot S. (2009) - Dramatic decrease of pelagic carbonate production by nannoplankton across the Early Toarcian anoxic event (T-OAE). *Global Planet. Change,* 65: 134-145.

Mattioli E., Plancq J., Boussaha M., Duarte L.V. & Pittet B. (2013) - Calcareous nannofossil biostratigraphy: new data from the Lower Jurassic of the Lusitatian Basin. *Comunicações Geológicas,* 100(Especial I): 69-76. Molfino B. & McIntyre A. (1990) - Precessional forcing of nutricline dynamics in the equatorial Atlantic. *Science*, 249: 766-769.

Mutterlose J., Bornemann A. & Herrle J. (2005) - Mesozoic calcareous nannofossils - state of art. *Palaontol. Z.,* 79(1): 113-133.

Muttoni G., Erba E., Kent D.V. & Bachtadse V. (2005) - Mesozoic Alpine facies deposition as a result of past latitudinal plate motion. *Nature,* 434: 59-63.

Noël D. (1965) - Sur les Coccolithes du Jurassique Européen et d'Afrique du Nord. *Edition du CNRS Paris*, 209 pp.

Olivier N., Pittet B. & Mattioli E. (2004) - Paleoenvironmental control on sponge-microbialite reefs and contemporaneous deep-shelf marl-limestones deposition (Late Oxfordian, Southern Germany). *Palaeogeogr., Palaeoclimatol., Palaeoecol.*, 212: 233-263.

Perch-Nielsen K. (1985) - Mesozoic calcareous nannofossil. In: Bolli H.M., Saunders J.B., Perch-Nielsen K. (Eds) - Plankton Stratigraphy: 329-426. Cambridge University Press, Cambridge.

Perilli N. (1999) - Calibration of Early-Middle Toarcian nannofossil events in two expanded and continuous sections from the Basque-Cantabrian area (Northern Spain). *Rev. Españ. Micropaleontol.,* 31(3): 393-401.

Perilli N. (2000) - Calibration of early-middle Toarcian nannofossil events based on high-resolution ammonite biostratigraphy in two expanded sections from the Iberian Range (East Spain). *Mar. Micropaleontol.,* 39: 293-308.

Perilli N. & Comas-Rengifo M.J. (2002) - Calibration of Pliensbachian calcareous nannofossil events in two ammonite-controlled sections from Northern Spain (Basque-Cantabrian area). *Riv. It. Paleontol. Strat.,* 108(1): 133-152.

Perilli N. & Duarte L.V. (2006) - Toarcian nannobiohorizons from Lusitanian Basin (Portugal) and their calibration against Ammonite Zones. *Riv. It. Paleontol. Strat.,* 112(3): 417-343.

Perilli N., Comas-Rengifo M.J. & Goy A. (2004) - Calibration of the Pliensbachian-Toarcian calcareous nannofossil zone boundaries based on ammonites (Basque-Cantabrian area, Spain). *Riv. It. Paleontol. Strat.,* 110(1): 97-107.

Perilli N., Fraguas A. & Comas-Rengifo M.J. (2010) - Reproducibility and reliability of the Pliensbachian calcareous nannofossil biohorizons from the Basque-Cantabrian Basin (Northern Spain). *Geobios,* 43(1): 77-85.

Picotti V. & Cobianchi M. (1996) - Jurassic periplatform sequences of Eastern Lombardian Basin (Southern Alps). The deep-sea record of the tectonic evolution, growth and demise history of a carbonate platform. *Mem. Soc. Geol.*, 48: 171-219.

Pittet B. & Mattioli E. (2002) - The carbonate signal and calcareous nannofossil distribution in an Upper Jurassic section (Balingen-Tieringen, Late Oxfordian, southern Germany). *Palaeogeogr. Palaeoclimatol. Palaeoecol.*, 179: 71-96.

Reale V. (1989) - Jurassic calcareous nannofossil and benthic foraminifera of the Valdorbia section. In: Cresta S., Monechi S. & Parisi G. (Eds) - Mesozoic-Cenozoic stratigraphy in the Umbria-Marche area. *Mem. Descr. Carta Geol. It.* 39: 80-88, Roma.

Reale V., Baldanza A., Monechi S. & Mattioli E. (1992) - Calcareous nannofossil biostratigraphic events from the Early-Middle Jurassic sequences of the Umbria-Marche area (Central Italy). *Mem. Sci. Geol.,* 43(allegato): 41-75.

Reggiani L., Mattioli E. & Pittet B. (2010a) - Spatial distribution of Late Pliensbachian (Early Jurassic) calcareous nannofossils within the Lusitanian basin (Portugal). *Geobios,* 43: 87-97.

Reggiani L., Mattioli E., Pittet B., Duarte L.V., Veiga de Oliveira L.C. & Comas-Rengifo M.J. (2010b) - Pliensbachian (Early Jurassic) calcareous nannofossils from the Peniche section (Lusitanian Basin, Portugal): a clue for paleoenvironmental reconstructions. *Mar. Micropaleontol.*, 75: 1-16.

Reolid M., Mattioli E., Nieto L.M. & Rodríguez-Tovar F.J. (2014) - The Early Toarcian Oceanic Anoxic Event in the External Subbetic (Southiberian Paleomargin, Westermost Tethys): Geochemistry, nannofossil and ichnology. *Palaeogeogr., Palaeoclimatol., Palaeoecol.*, 411: 79-94.

Roth P.H. (1983) - Jurassic and Lower Cretaceous calcareous nannofossil in the Western North Atlantic (Site 534): biostratigraphy, preservation and some observation on biogeography and paleoceanography. *Init. Rep. DSDP*, 76: 587-621.

Roth P.H. & Krumbach K.R. (1986) - Middle Cretaceous calcareous nannofossil biogeography and preservation in the Atlantic and Indian oceans: implications for paleoceanography. *Mar. Micropaleontol.*, 10: 235-266.

Sandoval J., Bill M., Aguado R., O'Dogherty L., Rivas P., Morard A. & Guex J. (2012) - The Toarcian in the Subbetic basin (Southern Spain): Bio-events (ammonite and calcareous nannofossil) and carbon-isotope stratigraphy. *Palaeogeogr., Palaeoclimatol., Palaeoecol.,* 342-343: 40-63.

Stover L.E. (1966) - Cretaceous coccoliths and associated nannofossils from France and the Netherlands. *Micropaleontology,* 12: 133-167.

Suan G., Mattioli E., Pittet B., Maillot S. & Lécuyer C. (2008) - Evidence for major environmental perturbation prior to and during the Toarcian (Early Jurassic) oceanic anoxic event from the Lusitanian Basin, Portugal. *Paleoceanography,* 23, PA1202, doi:10.1029/2007PA001459.

Suan G., Mattioli E., Pittet B., Lécuyer C., Sucheras-Marx B., Duarte L.V., Philippe M., Reggiani L. & Martineau F. (2010) - Secular environmental precursor to Early Toarcian (Jurassic) extreme climate changes. *Earth Planet. Sci. Lett.,* 290: 448-458.

Tiraboschi D. & Erba E. (2010) - Calcareous nannofossil biostratigraphy (Upper Bajocian-Lower Bathonian) of the Ravin du Bès section (Bas Auran, Subalpine Basin, SE France): Evolutionary trends of *Watznauria barnesiae* and new findings of "*Rucinolithus*" morphotypes. *Geobios,* 43: 59-76.

Tremolada F. & Erba E. (2002) - Morphometric analysis of Apian *Assipetra infracretacea* and *Rucinolithus terebrodentarius* nannoliths: implications for taxonomy, biostratigraphy and paleoceanography. *Mar. Micropaleontol.,* 44: 77-92.

Tremolada F., van de Schootbrugge B. & Erba E. (2005) - Early Jurassic schizosphaerellid crisis in Cantabria, Spain: implication for calcification rates and phytoplankton evolution across the Toarcian oceanic anoxic event. *Paleoceanography,* 20, PA2011, doi:10.1029/2004PA001120.

Tremolada F., Erba E., van de Schootbrugge B. & Mattioli E. (2006) - Calcareous nannofossil changes during the late Callovian - early Oxfordian cooling phase. *Mar. Micropaleontol.,* 59: 197-209.

Walsworth-Bell E.B. (2001) - Jurassic calcareous nannofossil and environmental cycles. Unpubl. Ph.D. Thesis, University College, London.

Wiegand G.E. (1984) - Two genera of calcareous nannofossils from the Lower Jurassic. *J. Paleontol.,* 58(4): 1151-1155.

Wignall P.B., Newton R.J. & Little C.T.S. (2005) - The timing of paleoenvironmental change and cause-and-effect relationships during the Early Jurassic mass extinction in Europe. *Am. J. Sci.,* 305: 1014-1032.

Winterer E.L. & Bosellini A. (1981) - Subsidence and sedimentation on Jurassic Passive Continental Margin, Southern Alps, Italy. *AAPG Bulletin,* 65: 394-421.

Young J.R., Tarquin Teale C. & Bown P.R. (1986) - Revision of the stratigraphy of the Longobucco Group (Liassic, southern Italy); based on new data from nannofossils and ammonites. *Eclogae Geol. Helv.,* 79: 117-135.

Appendix 1

Biscutum dubium (Noël 1965) Grün *in* Grün et al. 1974
B. finchii (Crux 1984) Bown 1987
B. grande Bown 1987
B. novum (Goy 1979) Bown 1987
Bussonius leufuensis Bown & Kielbowicz 1987
B. prinsii (Noël 1973) Goy 1979
Calyculus Noël 1973
Carinolithus cantaluppii Cobianchi 1990
C. poulnabronei Mattioli 1996
C. superbus (Deflandre 1954) Prins *in* Grün et al. 1974
Crepidolithus cavus Rood, Hay & Barnard 1973
C. crassus (Deflandre *in* Deflandre & Fert 1954) Noël 1965
C. granulatus Bown 1987
Diductius constans Goy 1979
Discorhabdus ignotus (Gorka 1957) Perch-Nielsen 1968
D. striatus Moshkovitz & Ehrlich 1976
Lotharingius barozii Noël 1973
L. crucicentralis (Medd 1971) Grün & Zweili 1980
L. frodoi Mattioli 1996
L. hauffii Grün & Zweili *in* Grün et al. 1974
L. sigillatus (Stradner 1961) Prins *in* Grün et al. 1974
L. umbriensis Mattioli 1996
L. velatus Bown & Cooper 1989
Mitrolithus elegans Deflandre 1954
M. jansae (Wiegand 1984) Bown *in* Young et al. 1986
M. lenticularis Bown 1987
Parhabdolithus liasicus Deflandre 1952
Rucinolithus Stover 1966
Schizosphaerella punctulata Deflandre & Dangeard 1938
Similiscutum cruciulus De Kaenel & Bergen 1993
Tubirhabdus patulus Rood et al. 1973
Watznaueria sp.1 Cobianchi et al. 1992

Taxonomic index of the calcareous nannofossil taxa reported in this study. Genera, species and subspecies are listed in alphabetic order. Authors and date of the original description and, when necessary, emendations are provided. See Bown (1987), Perch-Nielsen (1985), Bown & Cooper (1998), Mattioli & Erba (1999) and references therein for further information regarding taxonomy and authorship.

Appendix 2

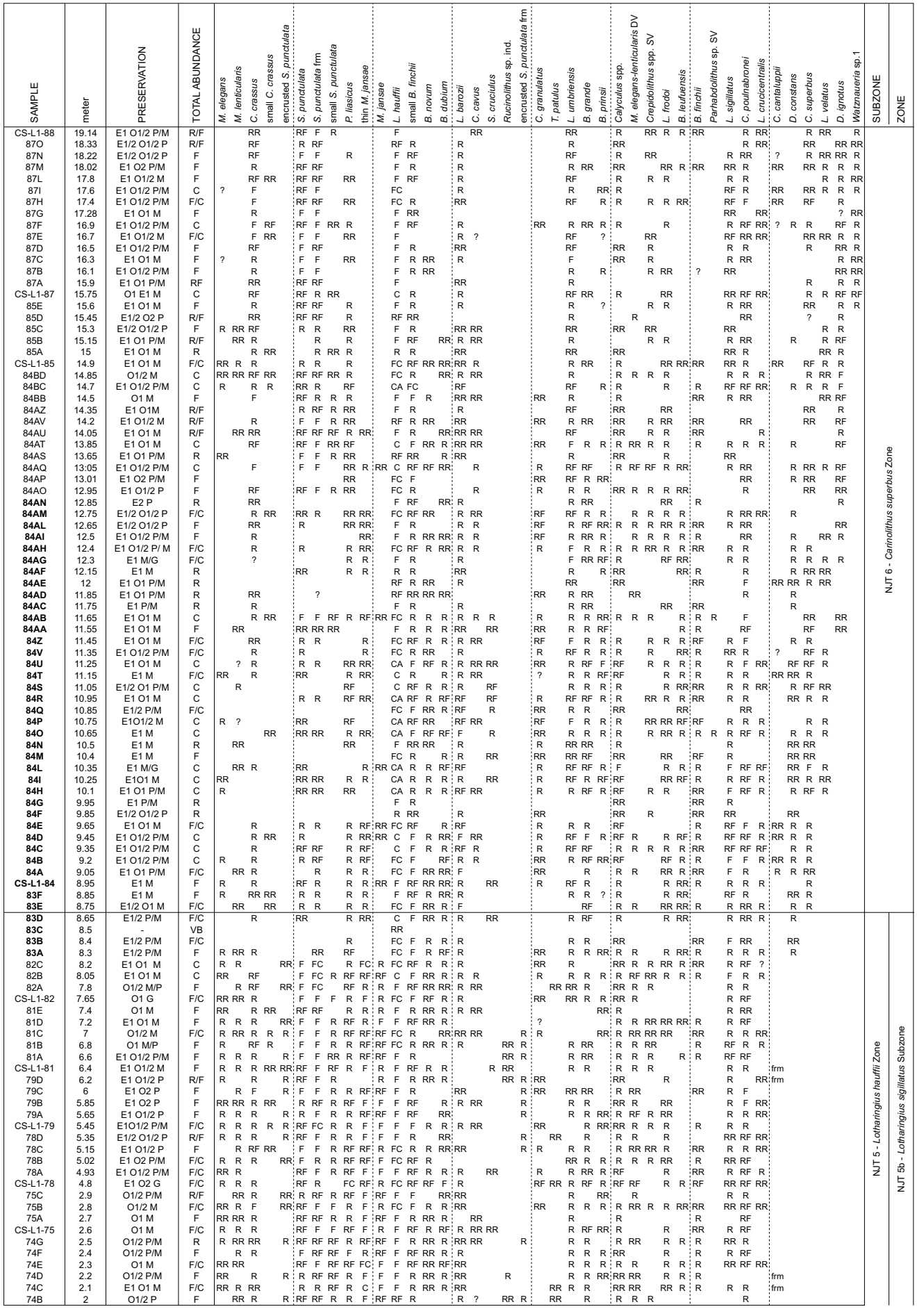
SAMPLE
meter
PRESERVATION
TOTAL ABUNDANCE
M. elegans
M. lenticularis
C. crassus
small C. crassus
encrusted S. punctulata
S. punctulata
S. punctulata frm
small S. punctulata
P. liasicus
thin M. jansae
M. jansae
L. hauffii
small B. finchii
B. novum
B. dubium
L. barozzii
C. cavus
S. cruciulus
Rucinolithus sp. ind.
encrusted S. punctulata frm
C. granulatus
T. patulus
L. umbriensis
B. grande
B. prinsii
Calyculus spp.
M. elegans-lenticularis DV
Crepidolithus spp. SV
L. frodoi
B. leufuensis
B. finchii
Parhabdolithus sp. SV
L. sigillatus
C. poulnabronei
L. crucicentralis
C. cantaluppii
D. constans
C. superbus
L. velatus
D. ignotus
Watznaueria sp.1
SUBZONE
ZONE
CS-L1-88 19.14 E1 O1/2 P/M R/F
87O 18.33 E1/2 O1/2 P R/F
87N 18.22 E1/2 O1/2 P F
87M 18.02 E1 O2 P/M F
87L 17.8 E1 O1/2 M F
87I 17.6 E1 O1/2 P/M C
87H 17.4 E1 O1/2 P/M F/C
87G 17.28 E1 O1 M F
87F 16.9 E1 O1/2 P/M C
87E 16.7 E1 O1/2 M F/C
87D 16.5 E1 O1/2 P/M F
87C 16.3 E1 O1 M F
87B 16.1 E1 O1/2 P/M F
87A 15.9 E1 O1 P/M RF
CS-L1-87 15.75 O1 E1 M C
85E 15.6 E1 O1 M F
85D 15.45 E1/2 O2 P R/F
85C 15.3 E1/2 O1/2 P F
85B 15.15 E1 O1 P/M R/F
85A 15 E1 O1 M R
CS-L1-85 14.9 E1 O1 M F/C
84BD 14.85 O1/2 M C
84BC 14.7 E1 O1/2 P/M C
84BB 14.5 O1 M F
84AZ 14.35 E1 O1M R/F
84AV 14.2 E1 O1/2 M R/F
84AU 14.05 E1 O1 M R/F
84AT 13.85 E1 O1 M C
84AS 13.65 E1 O1 P/M R
84AQ 13:05 E1 O1/2 P/M C
84AP 13.01 E1 O2 P/M F
84AO 12.95 E1 O1/2 P F
84AN 12.85 E2 P R
84AM 12.75 E1/2 O1/2 P F/C
84AL 12.65 E1/2 O1/2 P F
84AI 12.5 E1 O1/2 P/M F
84AH 12.4 E1 O1/2 P/ M F/C
84AG 12.3 E1 M/G F/C
84AF 12.15 E1 M R
84AE 12 E1 O1 P/M R
84AD 11.85 E1 O1 P/M R
84AC 11.75 E1 P/M R
84AB 11.65 E1 O1 M C
84AA 11.55 E1 O1 M F
84Z 11.45 E1 O1 M F/C
84V 11.35 E1 O1/2 P/M F/C
84U 11.25 E1 O1 M C
84T 11.15 E1 M F/C
84S 11.05 E1/2 O1 P/M C
84R 10.95 E1 O1 M C
84Q 10.85 E1/2 P/M F/C
84P 10.75 E1O1/2 M C
84O 10.65 E1 M C
84N 10.5 E1 M R
84M 10.4 E1 M F
84L 10.35 E1 M/G C
84I 10.25 E1O1 M C
84H 10.1 E1 O1 P/M C
84G 9.95 E1 P/M R
84F 9.85 E1/2 O1/2 P R
84E 9.65 E1 O1 M F/C
84D 9.45 E1 O1/2 P/M C
84C 9.35 E1 O1/2 P/M C
84B 9.2 E1 O1/2 P/M C
84A 9.05 E1 O1 P/M F/C
CS-L1-84 8.95 E1 M F
83F 8.85 E1 M F
83E 8.75 E1/2 O1 M F/C
83D 8.65 E1/2 P/M F/C
83C 8.5 - VB
83B 8.4 E1/2 P/M F/C
83A 8.3 E1/2 P/M F
82C 8.2 E1 O1 M C
82B 8.05 E1 O1 M C
82A 7.8 O1/2 M/P F
CS-L1-82 7.65 O1 G F/C
81E 7.4 O1 M F
81D 7.2 E1 O1 M F
81C 7 O1/2 M F/C
81B 6.8 O1 M/P F
81A 6.6 E1 O1/2 P/M F
CS-L1-81 6.4 E1 O1/2 M F
79D 6.2 E1 O1/2 P R/F
79C 6 E1 O2 P F
79B 5.85 E1 O2 P F
79A 5.65 E1 O1/2 P F
CS-L1-79 5.45 E1O1/2 P/M F/C
78D 5.35 E1/2 O1/2 P R/F
78C 5.15 E1 O1/2 P F
78B 5.02 E1 O2 P/M F/C
78A 4.93 E1 O1/2 P/M F/C
CS-L1-78 4.8 E1 O2 G F/C
75C 2.9 O1/2 P/M R/F
75B 2.8 O1/2 M F/C
75A 2.7 O1 M F
CS-L1-75 2.6 O1 M F/C
74G 2.5 O1/2 P/M R
74F 2.4 O1/2 P/M F
74E 2.3 O1 M F/C
74D 2.2 O1/2 P/M F
74C 2.1 E1 O1 M F/C
74B 2 O1/2 P F
NJT 6 - Carinolithus superbus Zone
NJT 5 - Lotharingius hauffii Zone
NJT 5b - Lotharingius sigillatus Subzone

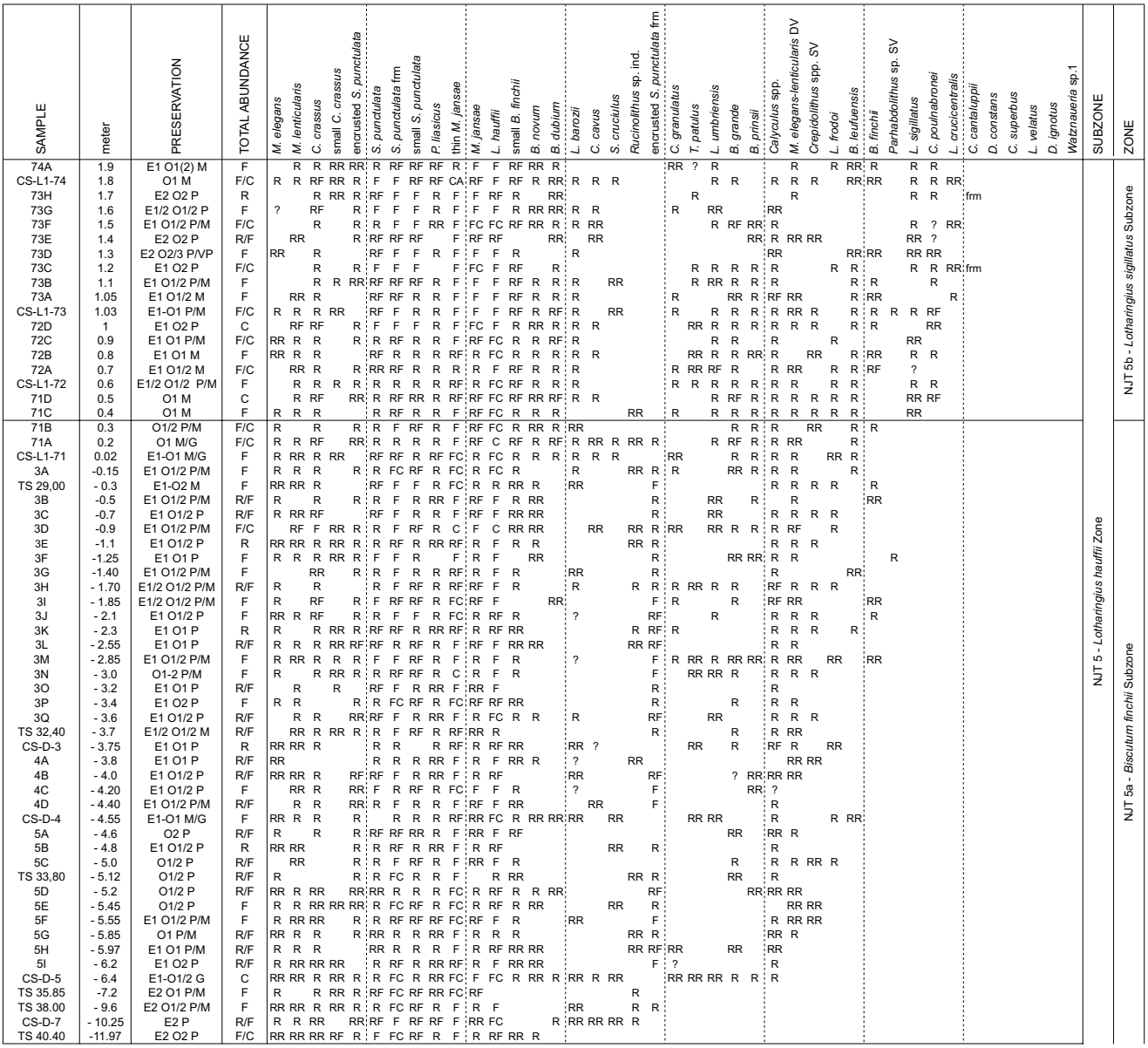

Calcareous nannofossil range chart of the Colle di Sogno section. The chart reports the distribution and semi-quantitative abundance of all taxa observed, as well as total abundance and preservation of each investigated sample. "?" corresponds to badly preserved specimens that cannot be unequivocally classified but are tentatively assigned to a taxon. "Frm" means fragment; "DV" means distal view; "SV" means side view. Total and semi-quantitative abundances obtained as follows:

Total abundance:

C/A (common to abundant): more than 11 specimens per field of view.

C (common): 6-10 specimens per field of view.

F/C (few/common): 1-5 specimens per field of view.

F (few): 1 specimen in 1-5 fields of view.

R/F (rare/frequent): 1 specimen in 6-10 fields of view.

R (rare): 1 specimen in 11-50 fields of view.

RR (very rare): 1 specimen in 51-100 fields of view.

VB (virtually barren): 1 specimen in more than 100 fields of view.

Abundance of individual taxa:

C/A (common/abundant): >30 specimens in 50 fields of view.

C (common): >30 specimens in 100 fields of view.

FC (few/common): >30 specimens in 200 fields of view.

F (few): 11-30 specimens in 200 fields of view.

RF (rare/few): 6-10 specimens in 200 fields of view.

R (rare): 1-5 specimens in 200 fields of view.

RR (extremely rare): 1 specimen in 400 fields of view.

Preservation of calcareous nannofossils was characterized adopting the codes described by Roth (1983): E1 (slight etching); E2 (moderate etching); E3 (strong dissolution); O1 (slight overgrowth); O2 (moderate overgrowth); O3 (strong overgrowth). Moreover preservation was also coded as follows:

- G (good): no evidence of dissolution and/or overgrowth; primary morphological characteristics are preserved.

- MG (moderate/good): very little evidence of dissolution and/or overgrowth; primary morphological characteristics are usually preserved.

- M (moderate): little evidence of dissolution and/or overgrowth; primary morphological characteristics are sometimes altered.

- MP (moderate/poor): evidence of dissolution and/or overgrowth; primary morphological characteristics are often altered.

- P (poor): most specimens exhibit dissolution or overgrowth; primary morphological characteristics are often destroyed.